

Composite I-Beam Fabrication and Testing in Response to 14th Annual SAMPE Bridge
Competition

A Senior Project

Presented to

the Faculty of the Aerospace Engineering Department
California Polytechnic State University, San Luis Obispo

In Partial Fulfillment

of the Requirements for the Degree

Bachelor of Science

by

Kodi Rider, Niño Noel Las Piñas and Hans Mayta

June 8, 2011

© 2011 Kodi Rider, Niño Noel Las Piñas and Hans Mayta

Composite I-Beam Fabrication and Testing in Response to 14th Annual SAMPE Bridge Competition

Kodi Rider¹, Niño Noel Las Piñas² and Hans A. Mayta³

Aerospace Engineering Dept., California Polytechnic State University, San Luis Obispo, CA 93410

Composites are a type of material that generally combines two materials yielding mechanical properties that are different than its constituent parts. These constituents are classified as either a fiber or a matrix. The objective of this project is to create a carbon-fiber composite I-beam that meets the specifications of the SAMPE student bridge competition. The I-beam consists of carbon fiber unidirectional and woven laminas, as well as aluminum honeycomb and high density polystyrene foam to stiffen the structure. The bridge contest rules limit the dimensions and weight of the bridge. The cross-section must be within 4 inches x 4 inches with a minimum length of 24 inches, and a maximum weight 600 grams. Theoretical stress and deflection analysis of the bridge was performed using MSC Nastran finite element software. All bridges were manufactured using a wet layup technique and cured under vacuum. Composite bridges were tested using the Instron machine belonging to the architectural engineering department at Cal Poly San Luis Obispo. Through analysis and testing, it was determined that web stability was the driving failure mode to design for. Our final bridge failed under 3000 lb_f due to buckling of the web directly beneath the applied load. Our first and fourth iterations saw twisting of the flanges because of the lack of stiffness in the flange structure. Our second bridge iteration had the highest strength-to-weight ratio and also took the highest load (3100 lb_f) before failing. Based on testing and performance at the SAMPE competition, there are many aspects of this project that can be improved, most importantly through manufacturing techniques. Use of an autoclave as well as using metal molds for curing the beam will dramatically increase load carrying capability.

¹ Undergraduate Student, Aerospace Engineering Dept., Cal Poly, krider@calpoly.edu.

² Undergraduate Student, Aerospace Engineering Dept., Cal Poly, nlaspi@calpoly.edu.

³ Undergraduate Student, Aerospace Engineering Dept., Cal Poly, hmayta@calpoly.edu

Introduction

Composites are a type of material that combines two or more different materials yielding a new material with mechanical properties that are different than its constituent parts. The constituents are classified as either a fiber or a matrix. Fibers are strands of homogeneous material that are typically laid out in unidirectional, woven, or veil configurations as shown in fig. 1.

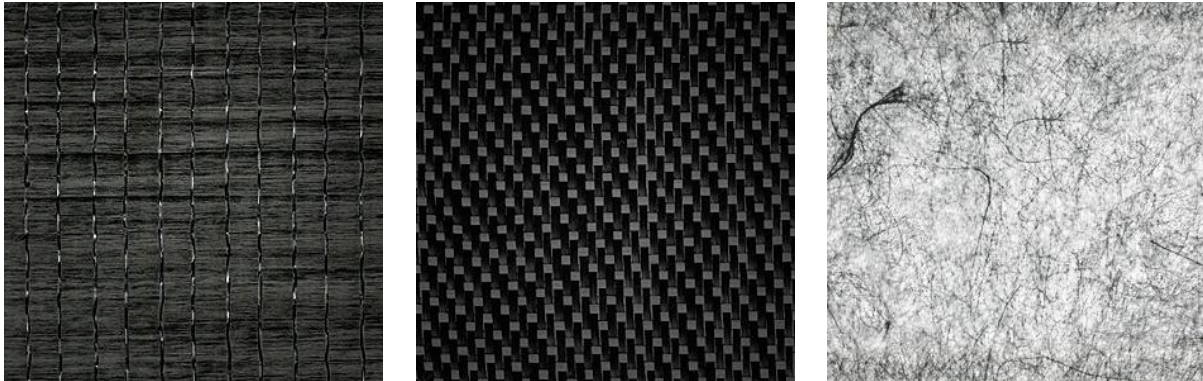


Figure 1. Composite fibers can have many orientations including unidirectional (left), woven (center), and veil (right).¹¹

The types of material that can act as fiber include carbon, aluminum, glass, graphite, boron, Kevlar, titanium, and steel. The fiber is encased in a matrix and acts as the main load bearing material. The purpose of the matrix is to hold the fibers together as they would otherwise separate. Matrix material includes cement, epoxy, polyester, carbon, and most metals. Composites are typically composed of one or more layers called lamina. The composite as a whole is called a laminate. An example of a composite material is fiberglass which can be commonly found in race car bodies.

If designed and fabricated well, composites are advantageous in that they inherit the strengths of their components as well as display high strength-to-weight and stiffness-to-weight ratios. Other properties that can be improved by forming a composite material are wear resistance, fatigue life, corrosion resistance, temperature-dependant behavior, acoustic insulation, thermal conductivity, and thermal insulation. In addition, composites can be molded to almost any shape and designed to exhibit the characteristics desired for its specific application. With these appealing qualities, composites have become widely used in, but not limited to, the design of aircraft and spacecraft in which weight minimization and material specialization is critical. Recently, Boeing unveiled its 787 Dreamliner

shown in fig. 2. Unlike conventional aircraft, more than 50% of its structure, including the fuselage and wings, is composed of composite materials.

Despite their advantages, composites do have a serious disadvantage that must be taken into account in the design of any composite containing structure. Composites are prone to mechanical damage that can destroy the load bearing fibers within the matrix. The destruction of a fiber creates a localized stress concentration that, if undetected, can propagate through the composite to the point of structural failure. Unlike homogeneous materials, this damage is not detectable by visual inspection but is rather concealed by the matrix material. Methods of damage detection include x-ray and ultrasound imaging.



Figure 2. Illustration of the Boeing 787-Dreamliner.¹⁰

There are several categories that matrix material can be classified under. These categories include thermosets, thermoplastics, organics, and non-organics. Thermoset materials are initially a low viscosity liquid but can be cured at atmospheric pressure and room temperature and faster at higher temperatures and higher pressures. An example of such a matrix is epoxy. An advantage of using a thermoset matrix is the relative ease of epoxy infusion during fabrication, even with complicated shapes and low pressures. Thermoplastics are materials that allow the composite to become plastic at high temperatures. An example of a thermoplastic is polyester. The advantage of using thermoplastics is the relative ease of molding the material since it can be placed in a cold mold while hot and then cured. Another advantage of using a thermoplastic is its ability to be recycled if damaged. Organic materials are materials whose molecular structure contains carbon-hydrogen bonds. One advantage of using an organic matrix is its thermal and electrical insulation properties. Non-organic materials do not contain carbon-hydrogen bonds. Typically, the bonds in a non-organic material are ionic or metallic. In opposition to organics, non-organics are good thermal and electrical conductors. Metal is a typical example of a non-organic matrix.

Numerous methods of fabricating a composite have been devised throughout the years with variations specific to the end application of the material. In general, composites start off as sheets of fiber material which form the basis of the lamina layers. These sheets of fiber are then infused with a desirably low viscosity matrix material. Curing of the material can be performed by either a hot press, a heated mold, or in an autoclave. A hot press is two

hot plates pressed together. A heated mold is a mold heated to cure the matrix. Finally, an autoclave is a vacuum chamber with a heating element that heats the composite to cure the matrix. Depending on the type of matrix material used, molding of the composite can be performed before or after curing. If a thermoset is used, the composite material must be in its desired shape while curing because it cannot be reverted to its post-cured shape. Alternatively, thermoplastics can be molded after curing by additional heating.

The objective of this project is to create a carbon-fiber composite I-beam that meets the specifications of the SAMPE student bridge competition. The I-beam consists of carbon fiber unidirectional and woven laminas, as well as aluminum honeycomb and high density poly styrene foam to stiffen the structure. The bridge contest rules limit the dimensions and weight of the bridge. The cross-section must be within 4 inches x 4 inches with a minimum length of 24 inches and a maximum weight 600 grams. Also, the maximum allowable width of the I-beam web is 0.6 inches. The construction of the preliminary I-beam serves as a learning experience to familiarize the group with the procedure to manufacture a composite I-beam and to refine the techniques that will be used to create the final I-beam for the contest. The first beam was created using wooden molds that allow the composite layers to be sandwiched together in the shape of an I-beam under the vacuum bagging as the resin is cured in the assembly.

Manufacturing Processes in Industry

There are three general layup processes for laminated fibrous composites: winding, laying, and molding. The most practiced winding and laying techniques are filament winding, tape wrapping, and cloth wrapping. Filament winding consists of passing a fiber through a liquid resin and then winding it on a madrel (usually a sand casting) that is removed through exposure to water¹. Tape laying consists of tape made of prepreg composite held together by a removable backing material. The tape is applied by unwinding and placing it in the desired shape. Finally cloth wrapping or winding is accomplished the same way tape laying, but is more inflexible and limited¹. Molding is accomplished by hand laying a composite that is compressed under elevated temperatures. Molding is the method of manufacture of composite plates in the aerospace structures lab at Cal Poly San Luis Obispo. As shown in fig. 3, in industry, tape laying is very popular for its ease of manufacture and is more flexible in process capabilities⁵.

There are many methods for curing composites once the layup process has been completed. Heated molds can be made, but are expensive and require time for manufacture. Hot presses and autoclaves can also be used for curing composites. A hot press works by forcing two heated plates together, and an



Figure 3. Automated tape laying is a popular choice of manufacture in industry.⁵

autoclave is a chamber that increases both the pressure and temperature to desired curing levels. Presented in fig. 4, autoclave molding is a modification of pressure-bag and vacuum-bag molding. This process produces denser, void free moldings because higher heat and pressure are used for curing².

Based on composite I-beam manufacturing research, there are two basic methods of I-beam fabrication, several composite skin lay-up methods and two methods of curing the I-beams. The I-beams are either fabricated by co-curing the flanges and web into one piece at a time or by separately curing the flange and



Figure 4. Autoclave molding is a modification of vacuum bag molding.⁴

web components of the I-beam and then bonding them together using an adhesive with or without laminated angle corner pieces. As for the two curing methods, either the expensive autoclave is used or the low-cost hot press is used to cure the I-beam specimen.

For the fabrication of the composite I-beam, the researched methods used composite materials like Ceiba carbon/ epoxy (T300H/91)⁶ and glass/epoxy (Eglass/914)⁶ for either co-curing or separately curing the several I-beam components. The first researched method, found in reference 6, used the co-curing method by pre-forming two C-channels made up of 12 plies and putting it together with two rectangular strips made up of 12 plies as shown in fig. 5. To fill the triangular void which is found between the flange and web areas on the C-channel sections, two ropes or tows⁶ of the same composite material where used to fill it.

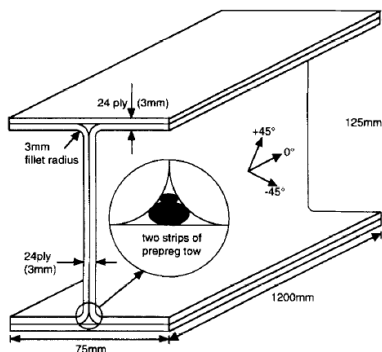


Figure 5. The 24-ply I-beam with the two C-channel sections, two flange caps, and the strips of wound prepreg tow.⁶

As for both the web and flanges of the I-beam of this researched method, the lay-ups contained an antisymmetric combination of $\pm 45^\circ$ and 0° plies, where the 0° direction is along the axis of the beam. To sustain the tensile and compressive loading existing within the beam flanges, the 0° plies were used in the design, and similarly, the $\pm 45^\circ$ layers were used in the web region to bear the shear loads. The multidirectional, 24-ply stacking sequence used in the first researched method was

$$45^\circ/0^\circ/45^\circ/-45^\circ/0^\circ/45^\circ/45^\circ/0^\circ$$

$$-45^\circ/45^\circ/0^\circ/-45^\circ/45^\circ/0^\circ/-45^\circ/45^\circ/0^\circ$$

$$-45^\circ/-45^\circ/0^\circ/45^\circ/-45^\circ/0^\circ/45^\circ/0^\circ$$

This stacking sequence minimized the number of coupling terms in the laminate stiffness matrix and minimized the interface moment stresses through the I-beam thickness.⁶ Finally, when the I-beam was co-cured, the preformed C-channel sections and the two flange strips were put into a mould and inserted into an autoclave.

The second I-beam manufacturing method, found in reference 7, used an I-beam structure design made up of two T-joints which had separate corner pieces, as shown in fig. 6. According to method two, the corner pieces strengthened the skin to spar web joint and allowed geometrical tolerances on the skin thickness and spar depth to be taken up in the assembly of the structure.⁷ The lay-ups for the two square composite flanges and web spar used different angled plies according to specific loading conditions.

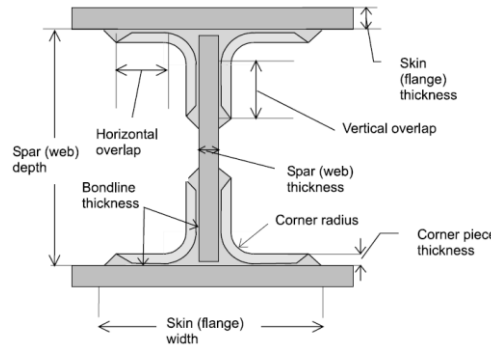


Figure 6. The geometry and structure of the 2nd researched method's I-beam.⁷

Since the two flanges experienced tension and compression, 0° plies were used along the axis of the beam. Similarly, to increase the buckling resistance of the flange beam, 60 percent of the plies were 0° , 30 percent were $\pm 45^\circ$, and 10 percent of the plies were 90° . As for the web spar, to avoid buckling caused by significant vertical compressive loads, the lay-up consisted of 10 percent of 0° plies, 30 percent of $\pm 45^\circ$ plies, and 60 percent made up

of 90° plies. After these composite skin lay-ups and I-beam components were fabricated manually, they were put together using an assembly tool shown in fig. 7 and cured with an autoclave.

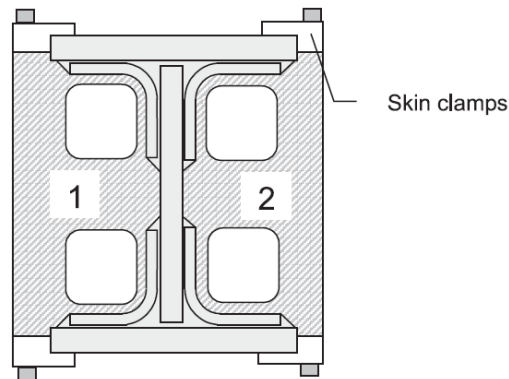


Figure 7. Schematic of the I-beam assembly tooling.⁷

The last researched method found in reference 8, used the co-curing method where both the flanges and the web are cured at the same time. According to the Zhou⁸ and Hood⁸, this fabrication method would save manufacturing time but also make the lay-up design extremely complicated. According to them, “If angle plies are involved”⁸ then both the flange and web laminates cannot have a symmetric lay-up at the same time. Also, instead of using an autoclave to cure the I-beam, a moulding piece design shown in fig. 8 was used to define the shape of the co-cured laminated I-beam which eased the fabrication and removal of the cured specimens. The hydraulic hot press used with the moulding device is shown in fig. 9 and is capable of delivering up to 2.1 MPa (300 psi) of pressure and temperatures up to 300 °C.⁸

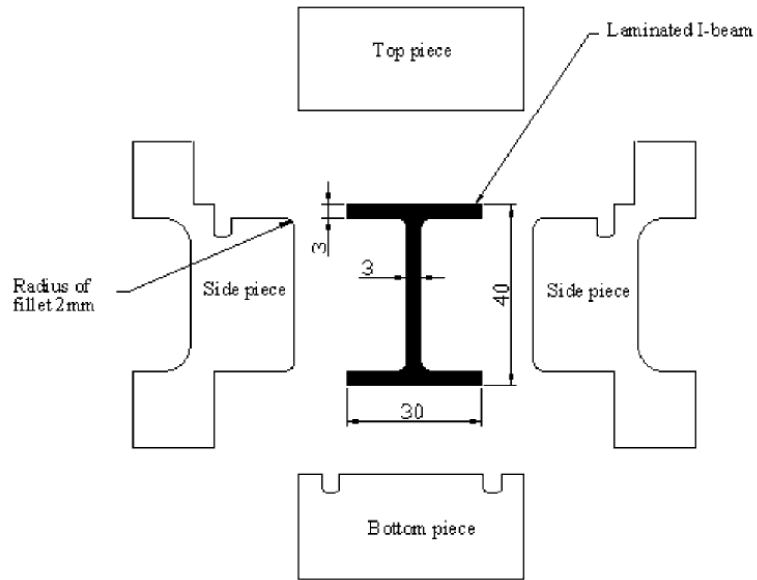


Figure 8. The unassembled schematic of the 4 piece mold used for fabricating the I-beam.⁸

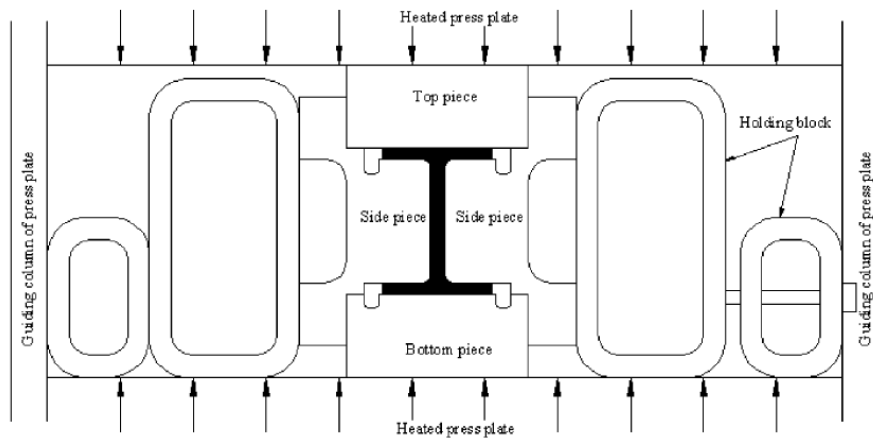


Figure 9. The schematic of the assembled 4 piece I-beam mold in the hot press.⁸

Theoretical Analysis

Theoretical stress and deflection analysis of the bridge was performed using MSC Nastran finite element software in conjunction with MSC Patran pre- and post-processing software. For comparison, multiple models were analyzed with different dimensions and different material properties. Dimensions were varied by web height in which three were modeled including a 4 inch web, 3 inch web, and a 2 inch web. With each differing cross section, four different model material properties were used: 7075 aluminum, 4130 steel, Ti 6Al-4V titanium, and woven carbon fiber. These materials were chosen because they are often used in industry for manufacture of various airplane components. The choice of these materials also allowed us to compare relative strength to weight ratios for each configuration to our experimental structures produced in lab. Theoretical mechanical properties (shown in Table 1) were obtained for each material and used in analysis.^{14 15 16 17}

Table 1. Theoretical mechanical properties used for finite element analysis.

Material	E ₁₁ (psi)	E ₂₂ (psi)	ν_{12}	G ₁₂ (psi)	G ₂₃ (psi)	G ₁₃ (psi)	ρ (lb/in ³)
7075 Aluminum ¹⁶	10400000		0.33				0.101
4130 Steel ¹⁴	29700000		0.29				0.284
Ti 6Al-4V Titanium ¹⁵	16500000		0.34				0.160
Woven Carbon Fiber ¹⁷	21900000	1460000	0.24	827000	493000	827000	0.050

Finite element models were meshed using Quad-4 elements with an Isomesh meshing technique. Each 2-dimensional element was specified as a 0.5 inch x 0.5 inch square. Roller constraints were placed 0.5 inches in from each end of the bridge and a symmetrical constraint was placed on the neutral axis along the center line of the bridge normal to the direction of loading. The roller constraints restricted displacement in the y- and z-directions while the symmetrical constraint restricted displacement in the x-direction. These boundary conditions were essential to fully constrain the model for analysis. A total load of 3000 lb_f was applied to a 4 inch x 4 inch section of the top flange of the bridge centered between the roller supports. This loading value was chosen as it was the best result seen during testing of the bridges. Figure 10 shows the meshed finite element model with the applied load and boundary conditions. Because the finite element mesh was specified as 2-dimensional, the thickness of both the web and the

flanges were defined with the material properties. The web was set to a thickness of 0.6 inches (the maximum allowed by the contest) and the each of the flanges was set a thickness of 0.25 inches, equivalent to the contest bridge.

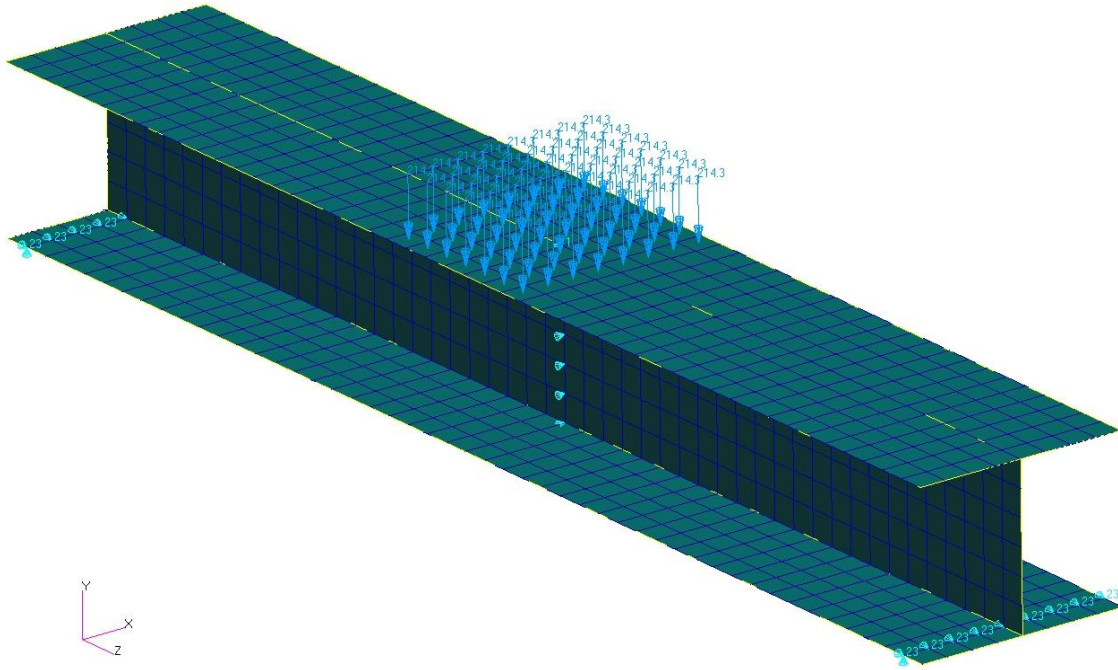


Figure 10. Meshed finite element model with load and boundary conditions applied.

Once the finite element model was created for each varying web height, static analysis was performed using MSC Nastran, and stress and displacement plots were generated for each material. Table 2 below shows the results from the finite element analysis for each material and web height. Refer to appendices A.1 through A.12 for full stress and displacement plots for each configuration.

Table 2. FEA maximum displacement and stress with differing materials and cross sectional areas.

Material	Web Height (inches)	Mass (g)	Maximum Stress (psi)	Maximum Displacement (inches)
7075 Aluminum	4	4842	15200	0.0257
	3	4182	15600	0.0295
	2	3522	17400	0.0421
4130 Steel	4	13616	15300	0.0090
	3	11759	15800	0.0104
	2	9902	17600	0.0147
Ti 6Al-4V Titanium	4	7671	15200	0.0161
	3	6625	15600	0.0168
	2	5579	17300	0.0265
Woven Carbon Fiber	4	2379	23600	0.0515
	3	2070	24000	0.0791
	2	1743	26000	0.1620

As the web height is decreased, maximum stress and displacement in the structure increases. This occurs because as the height of the structure decreases, the moment of inertia decreases. This transversely causes displacement to increase, which ultimately means an increase in stress. While decreasing the web height decreases the overall stiffness of the bridge, it increases the stability of the structure. After experimental testing and results from finite element analysis, it was determined that web stability was the driving failure mode to design for rather than the overall stiffness of the bridge. Figure 11 shows the displacement plot comparison of a 4 inch web bridge to a 2 inch web bridge made entirely from woven carbon fiber. Notice how deflection increases as the web height decreases.

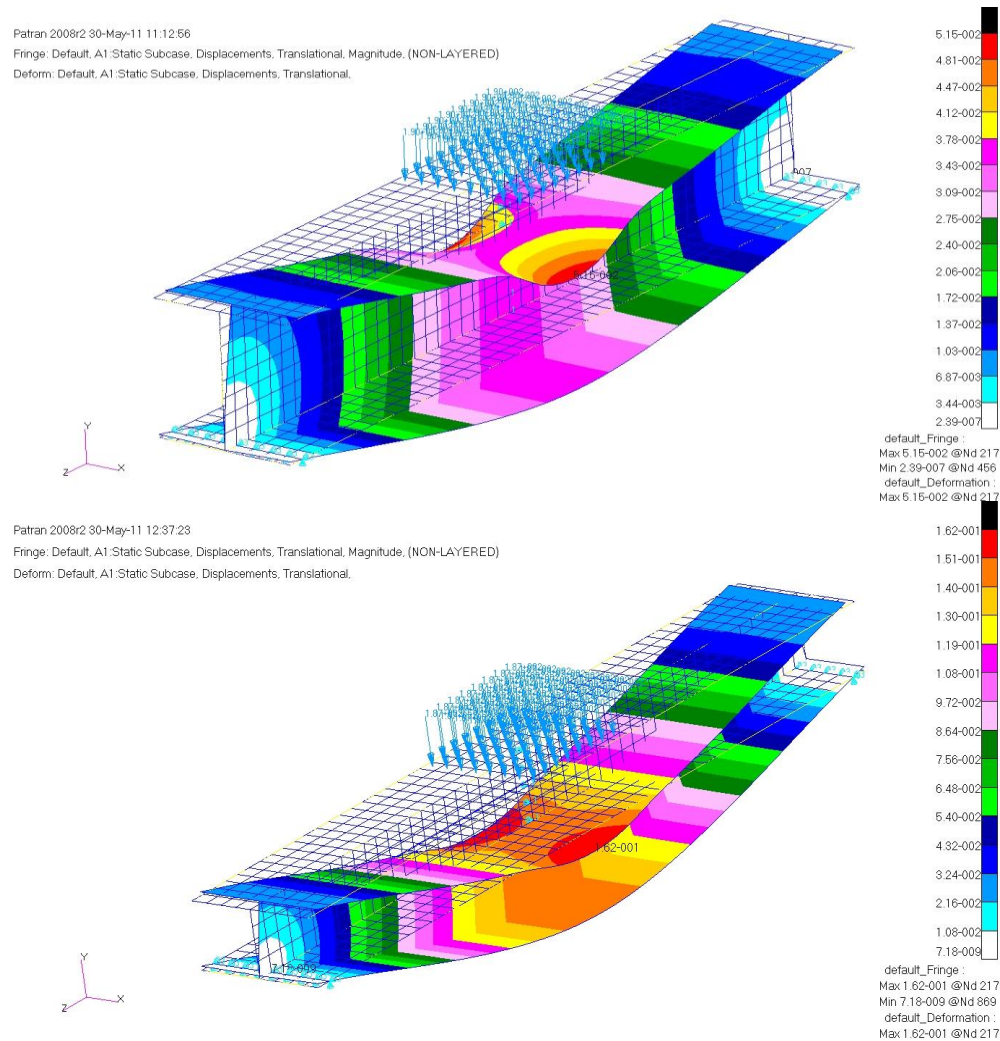


Figure 11. Finite element comparison of displacement as cross sectional area decreases.

Finite element analysis was compared to classical beam theory in order to validate the finite element model. An equation for maximum displacement was determined assuming a simply supported beam with a partially distributed uniform load as shown in fig. 12.

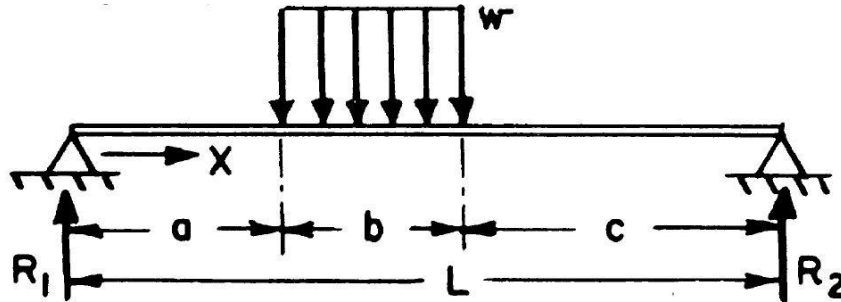


Figure 12. Theoretical model used to validate finite element model displacements.¹⁸

Where terms a and c are 9.5 inches, b is 4 inches, L is 23 inches, and w is 750 lb_f/in respectively. The classical beam theory displacements were then compared to finite element model displacements as shown in Table 3. Refer to appendix A.13 for classical beam theory calculations.

Table 3. Comparison of finite element analysis to classical beam theory calculations.

Material	Web Height (inches)	Theoretical Maximum Displacement (inches)	Finite Element Maximum Displacement (inches)	Difference (%)
7075 Aluminum	4	0.0235	0.0257	9.36
	3	0.0314	0.0295	6.05
	2	0.0434	0.0421	3.00
4130 Steel	4	0.0082	0.0090	9.76
	3	0.0110	0.0104	5.45
	2	0.0152	0.0147	3.29
Ti 6Al-4V Titanium	4	0.0148	0.0161	8.78
	3	0.0198	0.0168	15.15
	2	0.0273	0.0265	2.93

The finite element maximum displacements correlate closely with classical beam theory maximum displacements with deviations ranging from 3% to 15.15%. These differences occur due to the level of accuracy of each method. Finite element analysis took into consideration the entire 3 dimensional model and the interactions that occur between the web and the flanges. The classical beam theory analysis assumed that the bridge length was 23 inches, the distance between the roller supports. These assumptions result in the differences seen between finite element and classical beam theory analysis.

Design and Fabrication of Molds

The I-beam was created using a mold to maintain the shape of the beam while the lay-up was inside the vacuum bag. The molds consisted of a 4 inch x 4 inch wood beam that was cut down to a 26 inch length, and cut in half down the length to create two pieces. The cross section of these beams actually measured 1.75 inches x 3.5 inches so 0.25 inches of smooth particle board were connected using epoxy and small screws to the interior sides, the top, and the bottom of the half-sections to increase the cross-sectional area and to provide a smoother finish on the final product. These particle board sections were also cut down from a larger board, and were cut to minimize the gaps and the corners in the mold. The final product was two wooden pieces with smooth surfaces, and the cross-sectional shape desired, where the composites would be layered over the protective material and sandwiched between the molds.

The mold pieces were wrapped in protective layers of vacuum bagging, and packing tape to prevent the epoxy from seeping into the molds and to prevent the I-beam from adhering to the mold. The carbon fiber layers were placed in between the two side-by-side mold pieces with additional layers on the top and bottom of the mold to bond the sides together and create a uniform surface. This set-up was then placed in a vacuum bag and sealed. The vacuum pulled the entire set up together and sealed around the molds creating the I-beam shape.

This mold set up allowed the creation of a basic I-beam shape. However, the wood and particle board pieces compressed slightly under the vacuum so the overall cross-section came out smaller and distorted in places. The wooden beams in the molds were slightly warped to begin with so this also led to distortion in the composite beam. When the mold pieces were compressed in the vacuum, the alignment of the molds was skewed so the I-beams had other thickness differences and distortions in the beam.

The aforementioned molds were not used in later iterations of the I-beam, and instead a 3.5 inch x 3.5 inch x 5 foot piece of wood was used that was free of any noticeably distortions. Surface imperfections were present due to the wood grain but were deemed acceptable for manufacture.

The mold used to create the final contest I-beam was a 3 inch x 2 inch x 3 foot aluminum bar. This mold was used because final specifications called for a 3 inch high C-section.

Design and Fabrication of I-Beam

The initial fabrication method consisted of making the whole I-beam in one step. However, resin penetrating through to all the carbon fiber would be a problem, especially to the carbon fiber which would constitute the flange of the beam and is sandwiched between the molds during resin infusion. Consequently, it was decided to make one half of the I-beam first. For this step, only one of the mold blocks was needed. This block was prepared by first wrapping the block in green vacuum material and carefully taping it shut so that no resin during infusion would make contact with the block and otherwise ruin it as seen in fig. 13. Afterwards, a piece of flow media was cut to drape over the block as shown in fig. 14. The purpose of flow media is to create an



Figure 13. Mold wrapped with green vacuum bag.



Figure 14. Mold with green flow media.

easier path for the resin to flow through during infusion and lower the chance of barren spots in the carbon fiber. The flow media was cut to the exact length of the block. In addition, its width was sized so that, when draped over the block, it would cover one major side, cover the bottom and top side, and extend an inch past the edges. The next step was to cut two pieces of peel ply that are roughly the same size as the flow media shown in figure 15. The purpose of peel ply is to allow for easy removal of the composite from the mold once curing is completed. Soon after, a piece of pink vacuum bag material was cut. The piece of vacuum bag material had to be big enough to enclose the whole mold along with the carbon fiber, peel ply, and flow media. The next element of the mold to be prepared was the resin supply line. This supply line consisted of a spirally cut plastic tube sized to the length of the



Figure 15. Peel ply being applied to wooden mold.

was taking place, the pieces of carbon fiber needed were cut to size. The pieces needed consisted of one 8.5 inch x 26 inch woven carbon fiber and two 4 inch x 26 inch unidirectional carbon fiber with the larger dimension of the unidirectional

parallel to the running direction of the fibers. The carbon fiber, flow media, and peel ply were arranged with the mold in a manner shown in fig.17. In addition, the resin supply line and cotton material were laid parallel to the mold on opposite sides.

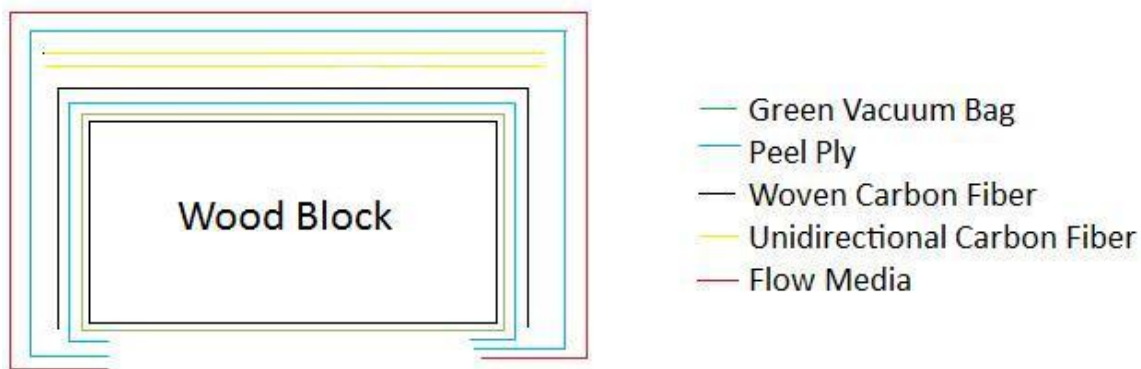


Figure 17. Carbon fiber layup, along with mold and materials used for curing.

After proper arrangement of the carbon fiber and all necessary pieces of the mold, everything was wrapped in the pink vacuum bag material with resin supply lines already attached to the t-connectors. The vacuum bag was sealed shut with yellow, double-sided gum tape. Extra care and attention had to be given when sealing the vacuum bag because sources of leaks are undesirable. After a satisfactory seal was created, a vacuum pump line was attached to the end opposite the resin supply line shown in fig. 18. The idea behind the location of the vacuum line is to pull the resin across the whole surface of the composite laminate while the vacuum is pulled. Before allowing resin to

block. Plastic t-connectors, which would later be connected to resin feed lines, were placed into the plastic tube shown in fig. 16. The final element of the mold to be cut was a long strip of cotton that will soak up any excess resin during infusion and curing.

While preparation of the mold

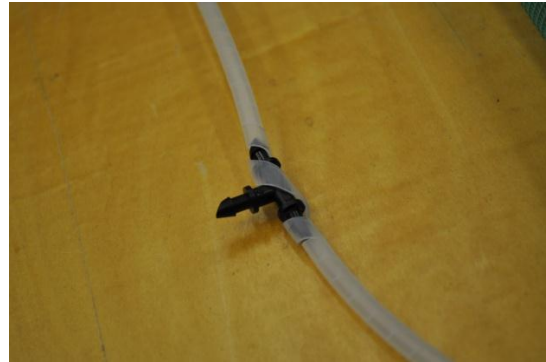


Figure 16. Vacuum hose with T-connector.

infuse, the resin feed lines were crimped with pliers and a vacuum was pulled to smoothen out any creases in the vacuum bag material. Any creases that are left alone will appear on the surface of the composite after curing. After all creases have been sufficiently smoothed out, the ends of the resin feed lines are attached to cups containing the resin and the lines are uncrimped to allow for suction of the resin into the mold. The resin mixture is 100 parts resin, 27 parts hardener, and the sum total of the mass of resin and hardener has to at least be equal to the mass of the carbon fiber. Additional hardener and resin mix



Figure 18. Assembly in vacuum bag with attachment of vacuum line.

was added to prevent running out of resin hardener mix. During resin infusion, extra attention had to be given to the resin level in the cups. Before the cup ran empty of resin, the feed line had to be crimped again to avoid suction of air into the mold. Once resin infusion was completed, the carbon fiber composite was left to cure overnight with the vacuum pump continuously running. The composite was removed the next day with care to avoid damage. As expected, the peel ply allowed for relatively easy removal of the composite from the mold.

With one half of the I-beam completed, the next process undertaken was to construct the rest of the I-beam. This process did not just involve creating another I-beam half. Rather, the rest of the I-beam was constructed from the already fabricated half using both molds. Once again, the wood molds had to be wrapped so that resin would not damage them during infusion. A different approach to protecting the molds was employed by completely wrapping them in packing tape. In addition, red plastic material was wrapped around the molds. After preparation of the molds, carbon fiber pieces were cut. These pieces consisted of three 8.5 inch x 26 inch woven, four 4.5 inch x 26 inch woven, three 4 inch x 26 inch unidirectional, and two 4.5 inch x 26 inch unidirectional with the larger dimension of the unidirectional parallel to the running direction of the fibers. Unlike the previous process, the pieces were infused with resin prior to placement on the molds. On one mold, one 8.5 inch x 26 inch woven piece was placed followed by the already constructed half and then by the three 4 inch x 26 inch unidirectional pieces as



Figure 19. Mold with half the I-beam, unidirectional fibers, and woven fibers.

shown in fig. 19. On the other mold, the remaining two 8.5 inch x 26 inch woven pieces were placed as shown in



Figure 20. Application of wet fibers to mold.



Figure 21. Assembled I-beam just before curing under vacuum.

fig. 20. Afterwards, both halves were put together as shown in fig. 21.

Once both halves were placed together, the first flange was created by placing a 4.5 inch x 26 inch unidirectional piece followed by two 4.5 inch x 26 inch woven pieces as shown in fig. 22. The other flange was created in the same manner. Upon completion of laying out the carbon fiber pieces, everything was wrapped in peel ply and sealed in a vacuum bag with preparations nearly identical to the previous process. The differences include not using the resin supply lines because the carbon fiber is already infused with resin and the whole assembly was further compressed with weights and clamps as shown in fig. 23. The sealed composite was left to cure overnight and removed once curing was completed. Once removed, the carbon fiber beam was cut down to a 24 inch length and the edges of the flanges were made as straight as possible using a band saw and dremel. The completed carbon



Figure 23. Application of wet flange pieces.



Figure 24. Bridge curing under vacuum with added weight.

fiber composite I-beam is shown in fig. 24.

The second version of the I-beam implemented aluminum honeycomb as the core of the web and flanges to increase stiffness and overall strength. Resin infusion of the carbon fiber in this version differs from the first version in that resin is not introduced by way of a resin supply line. Rather, the resin is pressed into the carbon fiber with a plastic putty knife before the carbon fiber is placed under vacuum to be cured. This method of introducing resin will be used

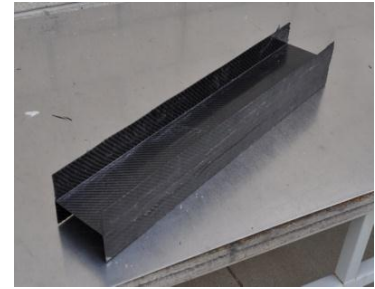


Figure 24. Completion of first I-beam.

for all future versions of the I-beam because it allows for more thorough distribution of the resin. This I-beam is composed of 5 independently cured pieces that were assembled in a final curing process. The constituent pieces of this I-beam are shown below in fig. 25.

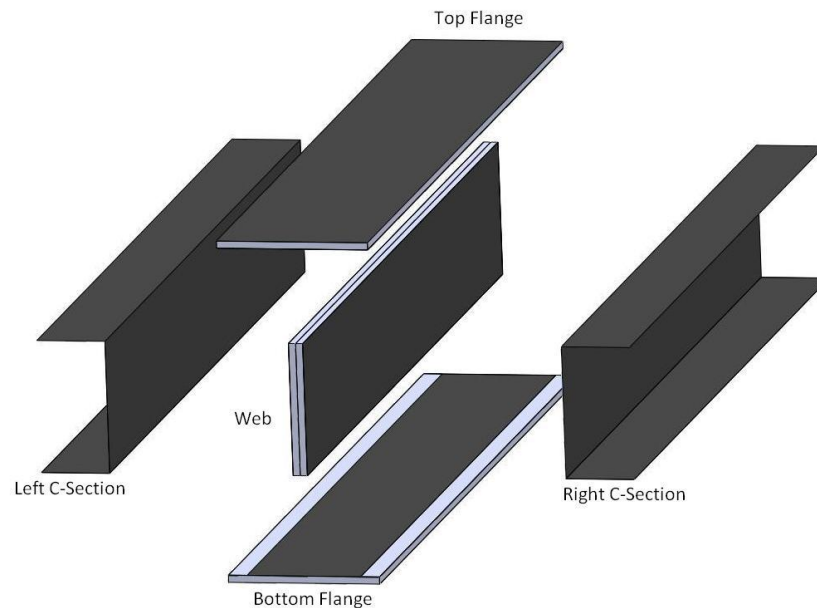


Figure 25. Exploded view of I-Beam version 2.

The left and right c-sections are composed of one layer of 0° unidirectional carbon fiber and one layer of 0° woven carbon fiber with the woven fiber as the surface layer. These pieces were fabricated as one long piece and then cut in half and trimmed. The mold for the C-sections was a 3.5 inch x 3.5 inch x 5 foot piece of wood. The wooden mold was protected by a layer of clear packing tape and an additional layer of porous plastic material. The carbon fiber was placed on the wooden mold and covered with a layer of release fabric first and then a layer of cotton to absorb excess resin. An additional strip of cotton was placed along the length of the wooden mold to allow

even vacuum distribution. The whole assembly was covered with a layer of green vacuum bag and sealed with gum tape. Before, the vacuum bag was completed sealed, the vacuum line was inserted while making sure to cover the opening with cotton to ensure that the line does not get plugged. The C-sections were left to cure for at least 12 hours. After curing, the C-sections were released and cut, using a tile saw, to the dimensions shown in fig. 26.

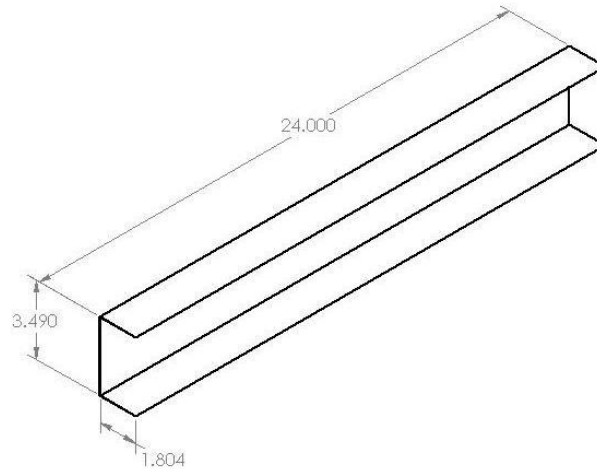


Figure 26. C-section dimensions in inches.

The top and bottom flanges have a core of aluminum 0.184 inch thick aluminum honeycomb sandwiched by layers of 0° unidirectional carbon fiber and 0° woven carbon fiber at the top with woven carbon fiber as the surface layer and 0° unidirectional carbon fiber at the bottom. The surface layer of woven carbon fiber is slightly wider than the core so that it wraps around the side edges to help prevent delamination. Construction of the flanges began by cutting the core and carbon fiber pieces to the exact widths and slightly longer than nominal dimensions. Next, resin is infused into the carbon fiber. A little more resin must be infused into the carbon fiber so that it will adhere better to the core. Afterwards, the core was sandwiched with the carbon fiber pieces. The whole assembly was then covered with a layer of release fabric. Cotton was omitted so that any excess resin is allowed to penetrate into the core for better adhesion of the carbon fiber to the core. Finally, the flanges are sealed in vacuum bag with gum tape, connected to a vacuum line, and left to cure overnight. While vacuum is forming in the bag, the edges of the vacuum bag were pressed to help make sure the carbon fiber is flush with the edges. After curing for at least 12 hours, the flanges were released and cut to length with a tile saw. The dimensions of the flanges are shown in fig. 27.

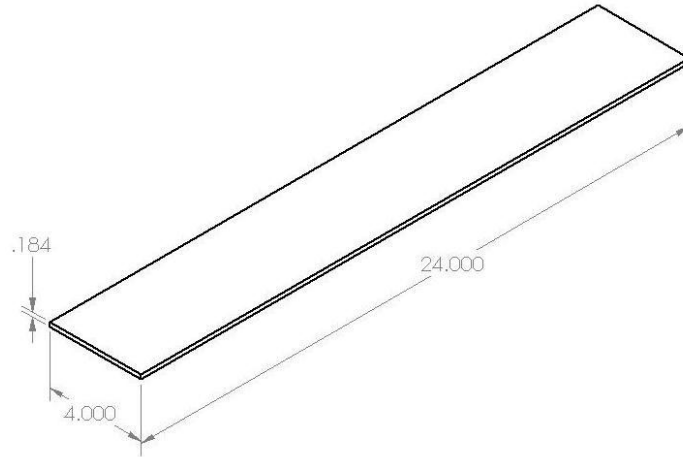


Figure 27. Flange dimensions in inches.

The web is composed of two layers of 0° unidirectional carbon fiber with aluminum honeycomb on either side which are then sandwiched one both sides with a layer 0° unidirectional carbon fiber and two layers of 0° woven carbon fiber. The process for manufacturing this piece is similar to that of the flanges except that all the pieces are initially cut slightly longer than their nominal dimensions and subjected to a finishing cut after curing. In addition, carbon fiber does not wrap around the edges. The dimensions of the core are shown below in fig. 28.

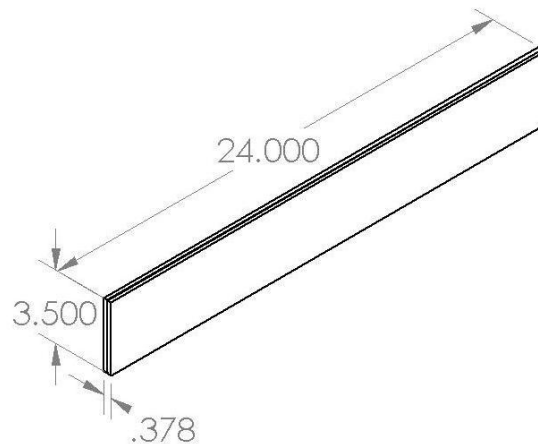


Figure 28. Web dimensions in inches.

The C-sections, web, and flanges were pieced together in a final curing process. A liberal amount of resin was applied to contact surfaces to help prevent dry spots during curing. The assembled I-beam was covered with a layer of release fabric as well as a layer of cotton. The assembly was wrapped in vacuum bag and connected to a vacuum line. A partial vacuum was first applied so that the wooden molds used to create the C-sections can be

placed in the C-sections to maintain the shape of the I-beam during curing. Vacuum was fully applied after the wooden molds were in place and the assembly was inspected to make sure that the pieces are oriented properly. Clamps were applied to the wooden molds and weights were placed on top of the I-beam assembly to better the bond between the individual pieces of the I-beam. This process of final I-beam assembly curing will be implemented for all future I-beam iterations

The third version of the I-beam differed from the second version in manufacturing process and materials only in that the web is not uniform throughout its length. Rather, solid carbon fiber pieces were built into either ends and trusses were built into the web. Otherwise, the C-sections and flanges are identical. An exploded view of the web is shown below in fig. 29.

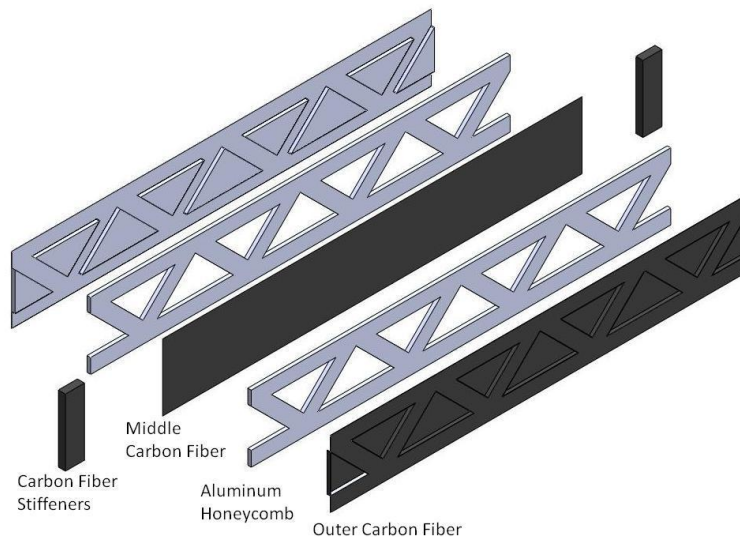


Figure 29. Exploded view of version 3 I-Beam web.

The solid end pieces were made from a solid plate of 50 layers of 0° woven carbon fiber. In the middle are two layers of 0° woven carbon fiber. On both sides of the web are one layer of 0° woven carbon fiber followed by a layer of 0° unidirectional carbon fiber and 0° woven carbon fiber.

Manufacturing of the web began by cutting pieces of aluminum honeycomb to shape except that the total length and width is slightly larger than nominal. The middle carbon fiber is also cut slightly larger than nominal. The outer layers must be cut to dimensions that take into account the amount of carbon fiber needed to recess into the triangular cutouts of the core. All the pieces of the web are assembled and sealed in a vacuum bag with a surrounding layer of release fabric first and then cotton. Before applying vacuum, the triangular pieces from the

cutouts of the core were fitted into the triangular cutouts from the outside of the vacuum bag. This was to ensure that, when vacuum was pulled, the recessing carbon fiber met in the middle of the web. After fitting the triangular pieces, full vacuum was applied and the web was left to cure for at least 12 hours. After curing, the web was released from the vacuum bag and trimmed to nominal dimensions using a tile saw.

The fourth version of the I-beam differed from the third version in that the truss shaped web is neglected in favor of a solid web. However, the same solid end pieces were still employed at the ends. In addition, the honeycomb core and middle layer of carbon fiber were replaced with a single thick piece of foam. Without triangular cutouts in the web, there is no need to use the triangular pieces used for the version three I-beam web. Otherwise, manufacturing of the web is similar to version three.

Another key difference in the fourth version of the I-beam is core material was neglected in the flanges. Rather, the flanges are solid pieces of carbon fiber. The mass of the omitted aluminum honeycomb core was substituted with approximately the same mass of carbon fiber. With the flanges purely carbon fiber, there was no need to cure them separately. Instead, the carbon fiber that would constitute the flanges was cured in the final I-beam assembly curing.

The fifth version of the I-beam took aspects of all the previous I-beam iterations. The flanges are identical to the flanges of the second and third version. The C-section is made of the same materials as in the second, third, and fourth version, and manufactured the same way. However, the height of the C-sections was reduced to 3 inches. As a result, the same wooden molds used in the previous versions could not be used. Instead, 3 inch x 2 inch 3 foot aluminum bars were used. The length of the aluminum bars did not allow for concurrent curing of both C-sections so both had to be cured separately. The web of the I-beam is similar to the fourth version; however, the foam core was replaced with higher density foam. In addition, woven carbon fiber spars that run along the length of the web were placed at the top and bottom on both sides of the foam. Shallow grooves with a depth equal to the thickness of the spars were cut into the top and bottom of the foam so that the surface of the spars is flush with the surface of the foam. An exploded view of the web is shown in fig. 30.

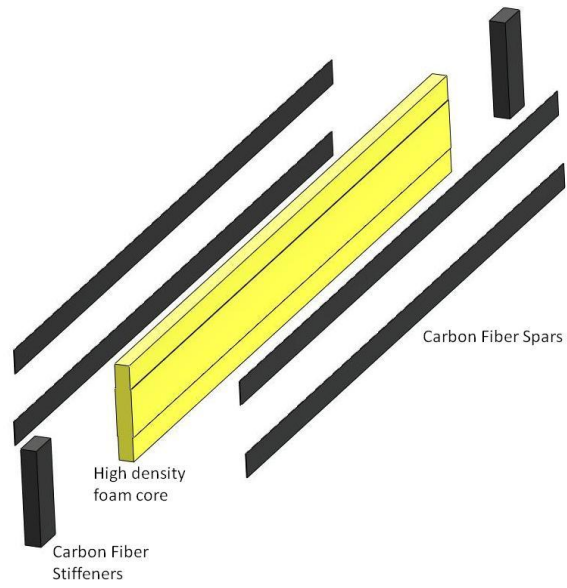


Figure 30. Exploded view of version 5 I-beam web

Experimental Test

Composite bridges were tested using the Instron machine belonging to the architectural engineering department at Cal Poly San Luis Obispo. We chose to use this machine because the Instron machine located in the aerospace structures lab was not large enough to test the 24 inch bridges. Testing of all 4 experimental iterations was performed using the architectural engineering Instron machine with assistance from the lab technician. Each bridge was tested under contest conditions, with roller supports spaced 23 inches apart and a 4 inch x 4 inch metal plate placed on the top flange centered on the bridge to distribute the loading by the machine, as shown in fig. 31. Figure 32 shows the Instron machine loaded with a bridge under contest conditions at Cal Poly.

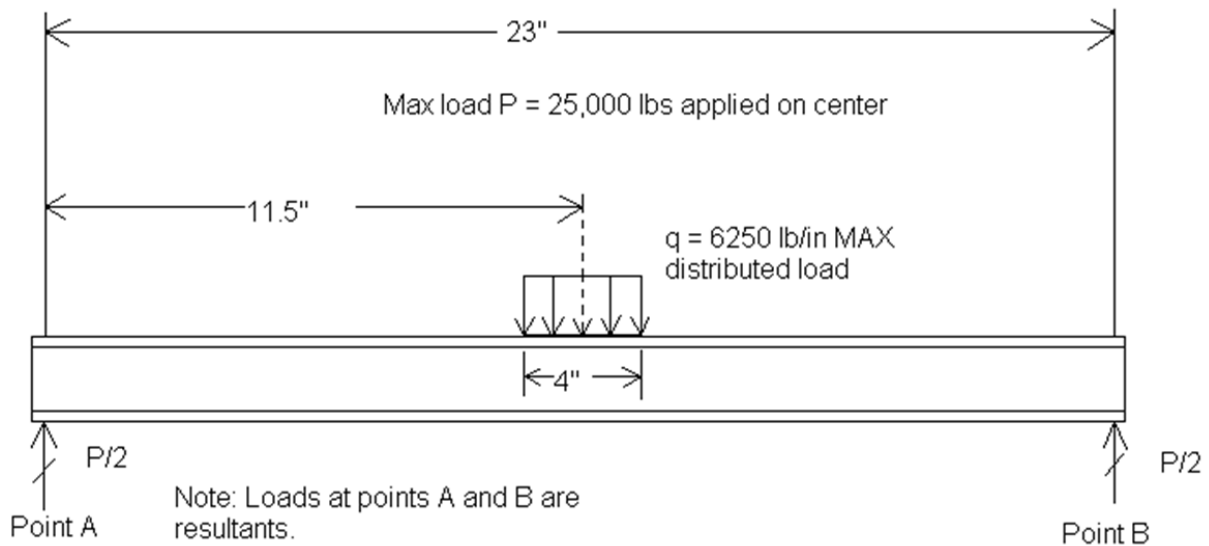


Figure 31. Free body diagram of bridge loading.



Figure 32. Bridge loaded under contest conditions at Cal Poly.

Experimental Resultants and Discussion

Testing began with our first bridge that was manufactured entirely out of carbon fiber and epoxy resin. As the bridge was loaded, both the upper and lower flanges began to twist between the roller supports. Failure due to buckling in the web occurred when the bridge was loaded to 2100 lb_f. This Buckling was localized to each end of the bridge just above where the roller support contacted the bridge. The bridge failure mode is shown below in fig. 33.

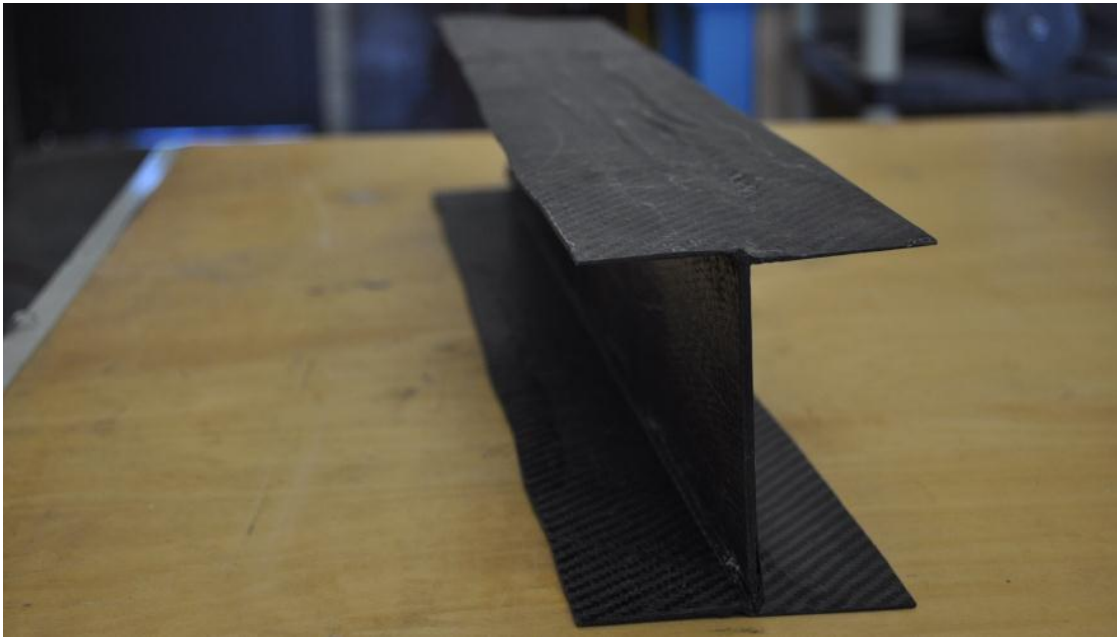


Figure 33. First iteration failure due to buckling in the web.

After testing our first bridge, we took into consideration the advantages and disadvantages of the design. Besides the twisting of the flanges, there was no noticeable bending in the direction of loading. This meant that web stability was the driving failure mode to design for. In order to increase the web stability and the overall stiffness of the beam, the cross sectional area had to be increased. This meant increasing the thickness of the flanges and web because the maximum allowable cross section dimensions were 4 inches x 4 inches. In order to increase the moment of inertia without significantly increasing weight, aluminum honeycomb core was used in both the flanges and the web.

Upon testing, our second bridge failed due to web buckling in the same location but was able to sustain 3100 lb_f before failing. The significant increase in load carrying capability of our second iteration drove us to use core material in all of our subsequent designs. As shown in fig. 34, buckling in the flange occurred above the roller support contact which was the same failure location as our first iteration. This meant that supporting the web on each end above the roller support was vital for mitigating localized buckling.

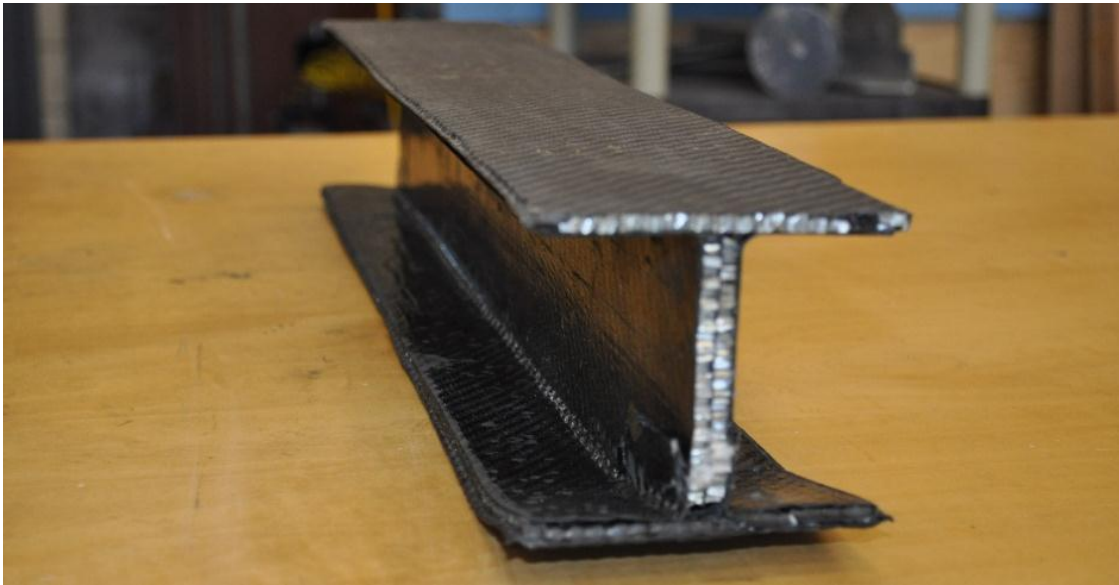


Figure 34. Second iteration failure due to buckling in the web.

Our third iteration included solid carbon epoxy columns on each end of the bridge in order to significantly stiffen the structure at the supports. These supports were made with 50 woven carbon layers. During testing of our third bridge, buckling at the ends did not occur due to the solid carbon fiber stiffeners. Failure still occurred in the web, but this was due to delamination of composite from the foam core as shown in fig. 35. Failure due to web delamination occurred when loading the bridge to 1750 lb_f.

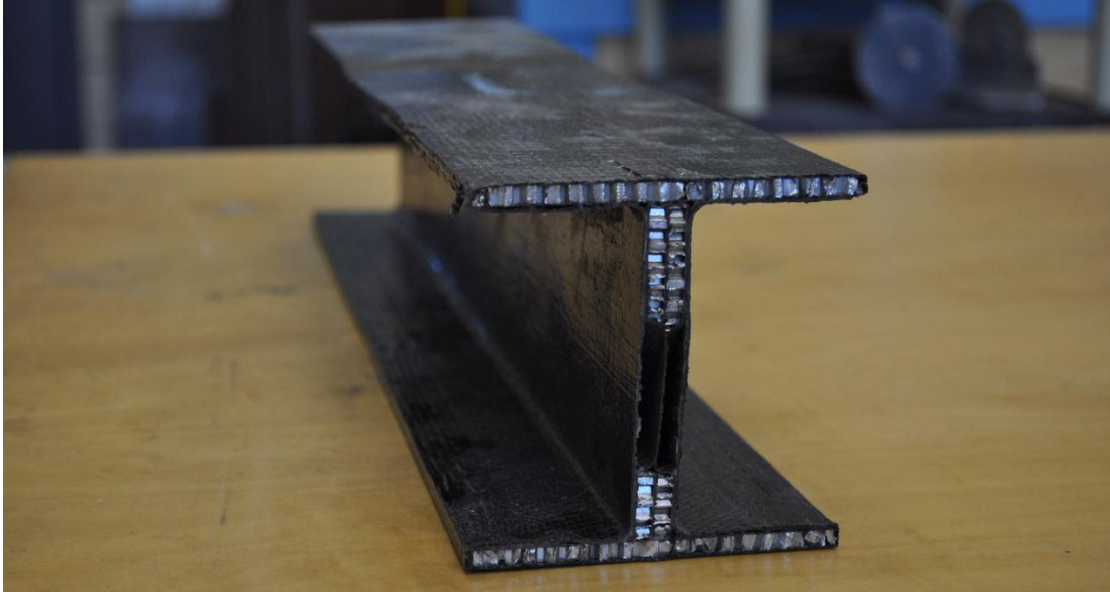


Figure 35. Third bridge iteration with solid carbon supports removed.

The delamination of the web in our third iteration was due to a lack of bonding area between the carbon fiber and the aluminum honeycomb. To remedy this, we decided to use high density polystyrene foam core for the web. In order to prevent buckling in the web, we used more layers of carbon fiber while still employing the use of the carbon fiber edge stiffeners. In this design, it was decided not to use aluminum honeycomb in the flanges because it did not provide more web stability. During testing of the 4th bridge, as shown in fig. 36, both the upper and lower flanges began to twist between roller supports, just as the 1st iteration had. We attributed this to a lack of torsional stiffness in the flanges, which was a direct effect to removing the aluminum honeycomb. Failure of the bridge occurred at 1675 lb_f due to composite delamination from the foam core.

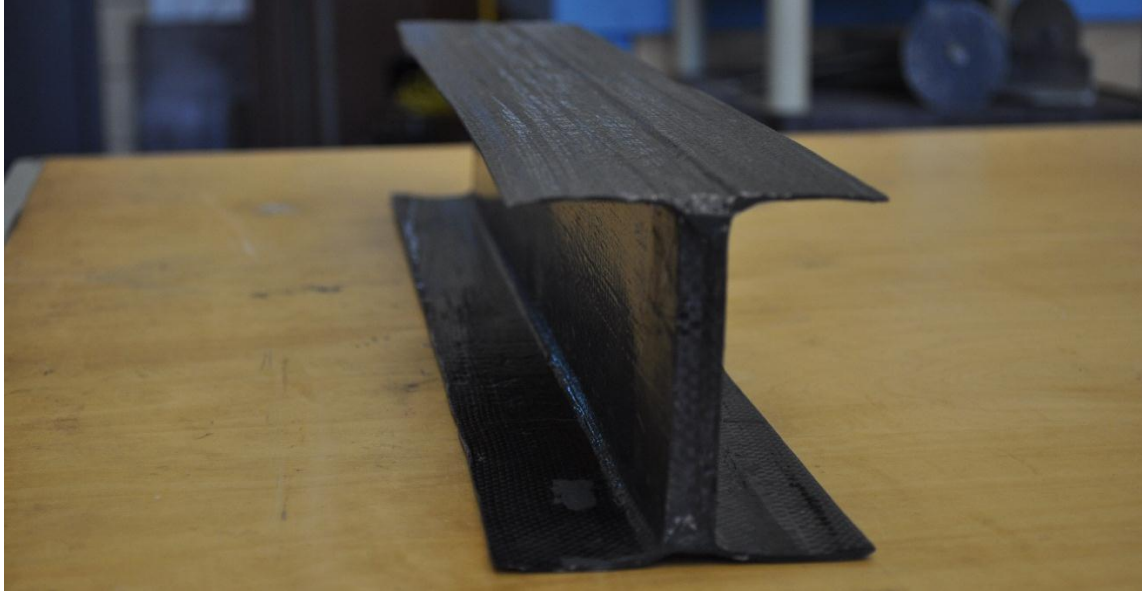


Figure 36. 4th bridge iteration with no aluminum honeycomb in the flanges.

With the different failure modes seen during testing, we were able mitigate these in our design for the contest bridge. Our final design included aluminum honeycomb cores in the flanges to prevent bridge twisting between the roller supports, solid carbon fiber columns on each end to prevent localized web buckling at the supports, and high density foam core in the web to maximize bonding and prevent fiber delamination. At the contest, our final design failed due to buckling in the web directly beneath an applied load of 3000 lb_f.. Figure 37 shows the failure mode of the bridge, with crack propagation carrying entirely down the length web.

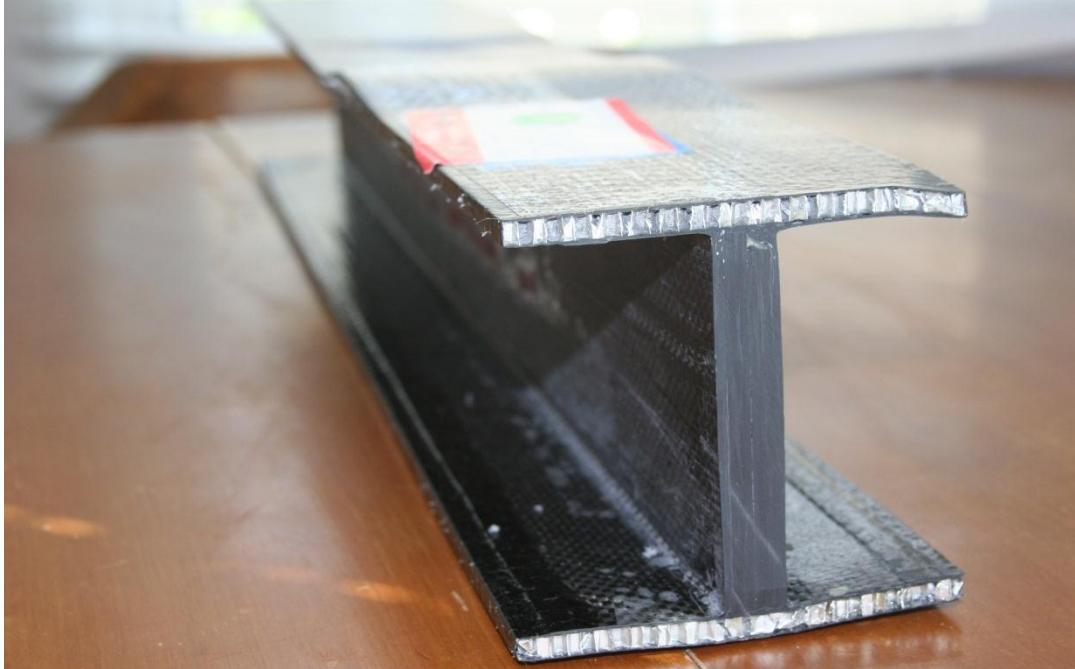


Figure 37. Test contest bridge that failed due to web buckling directly under the load contact.

Our final bridge was successful in that we were able to mitigate all of the failure modes experienced during pre-contest testing. Failure of this bridge occurred where the highest stress levels are seen under loading which follows with the theoretical finite element models produced. Table 4 shows the mass, ultimate load, and failure mode of each bridge produced during testing.

Table 4. Mass, ultimate load, and failure mode of all tested bridges.

	Mass (g)	Ultimate Load (lb _f)	Failure Mode
1 st Iteration	670	2100	Web Buckling at Ends and Flange Twisting
2 nd Iteration	594	3100	Web Buckling at Ends
3 rd Iteration	570	1900	Web Core Delamination
4 th Iteration	542	1675	Web Core Delamination and Flange Twisting
Contest Bridge	595	3000	Web Buckling at Center

Conclusion

Through analysis and testing, it was determined that web stability was the driving failure mode to design for and mitigate. Theoretical analysis showed that as the web height decreased, the overall stiffness of the structure decreased. This coupled with testing results showed that the web buckling occurred far before failure due to maximum allowable stress of the material. Through testing we were able to mitigate localized failures at the roller supports and twisting of the flanges. The final bridge failed where the highest stress levels are seen in the structure, which follows with theoretical finite element analysis. The first and fourth iterations saw twisting of the flanges because of the lack of stiffness in the flange structure. The second bridge iteration had the highest strength-to-weight ratio and also took the highest load before failing. All bridges were manufactured using a wet layup technique and cured under vacuum. This technique was found to be most effective for manufacturing the bridges. Earlier attempts using resin transfer infusion yielded a part with uneven resin content and air bubbles. The use of an aluminum mold also improved the quality of the part as opposed to using wood.

Based on testing and performance at the SAMPE competition, there are many aspects of this project that can be improved. A top priority is making metal molds for shaping and curing the bridge. This would provide a stiff molding structure that would not deform under vacuum and transfer heat well throughout the part during curing. Improving the method of manufacturing is another top priority. Many of the strongest bridges at the competition were cured using an autoclave. This creates a part with low matrix content which makes it stronger, cleaner, and containing less stress concentrations. The use of an autoclave would greatly improve the strength of the bridges manufactured. Besides improving the method of manufacture, understanding the driving failure modes to design for is also very important. Future improvements to the design of these bridges include more finite element analysis as well as determining the mechanical properties of the materials. Designing for web buckling will greatly improve bridge, and this can be done using finite element nonlinear buckling solutions. These improvements would dramatically increase the load carry capability of bridges.

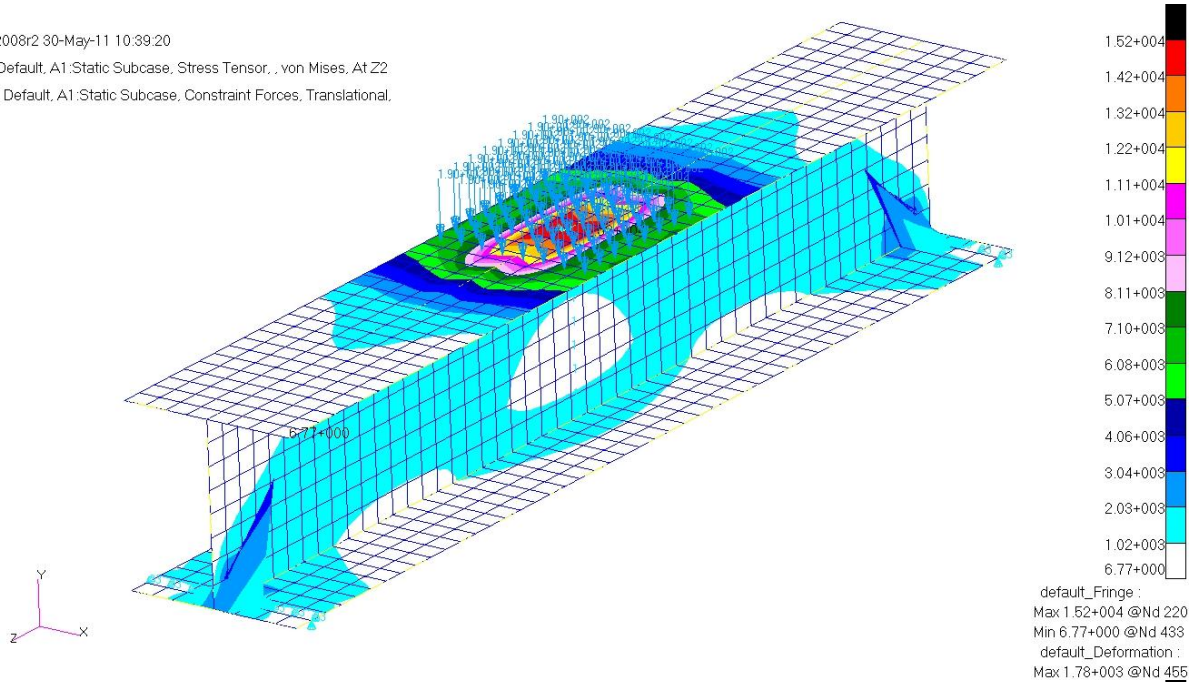
Appendix

Appendix A.1 – Stress and Displacement Plots of Finite Element Model with 7075 Aluminum and 4 Inch Web

Patran 2008r2 30-May-11 10:39:20

Fringe: Default, A1:Static Subcase, Stress Tensor, , von Mises, At Z2

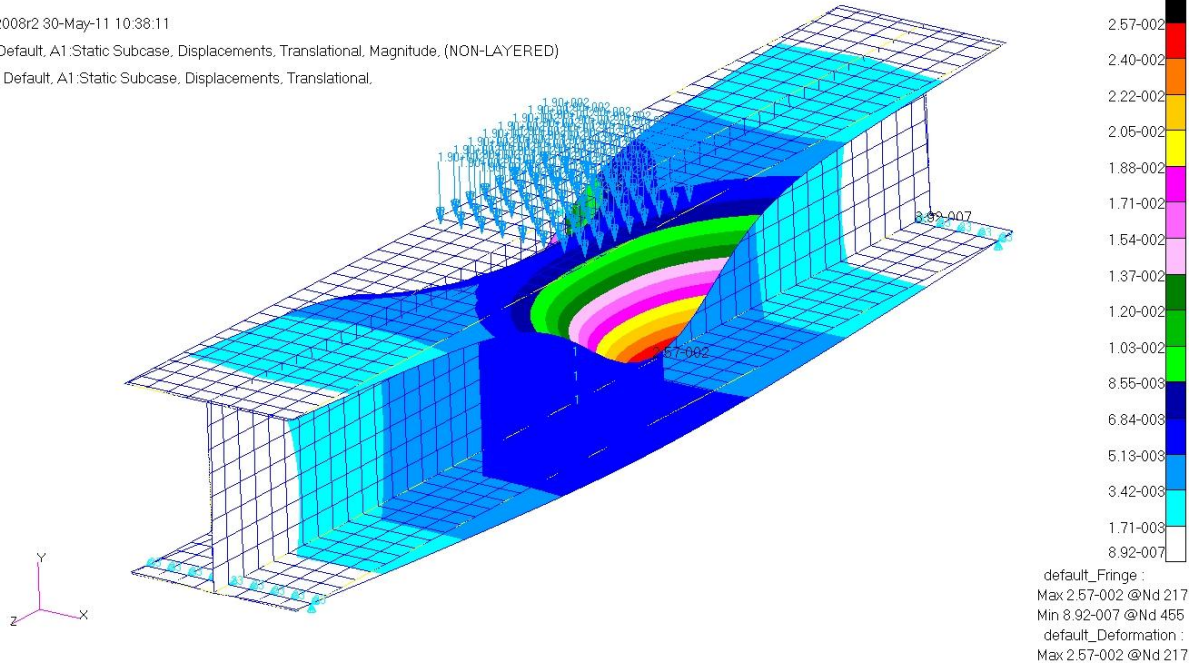
Deform: Default, A1:Static Subcase, Constraint Forces, Translational,



Patran 2008r2 30-May-11 10:38:11

Fringe: Default, A1:Static Subcase, Displacements, Translational, Magnitude, (NON-LAYERED)

Deform: Default, A1:Static Subcase, Displacements, Translational,

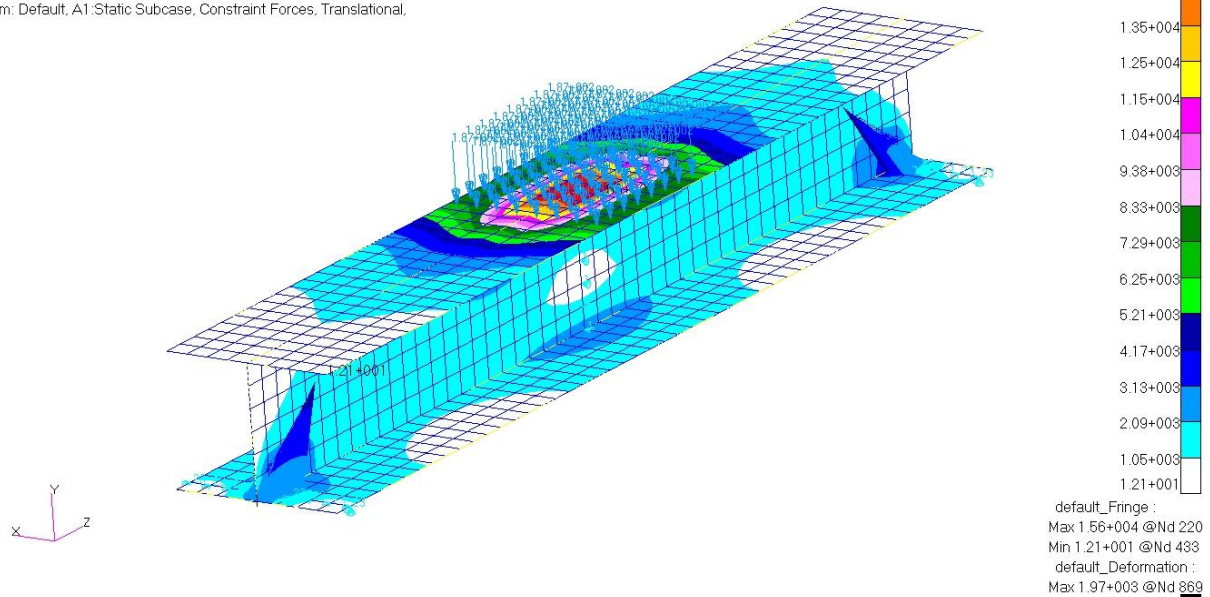


Appendix A.2 – Stress and Displacement Plots of Finite Element Model with 7075 Aluminum and 3 Inch Web

Patran 2008r2 30-May-11 11:42:21

Fringe: Default, A1:Static Subcase, Stress Tensor, von Mises, At Z2

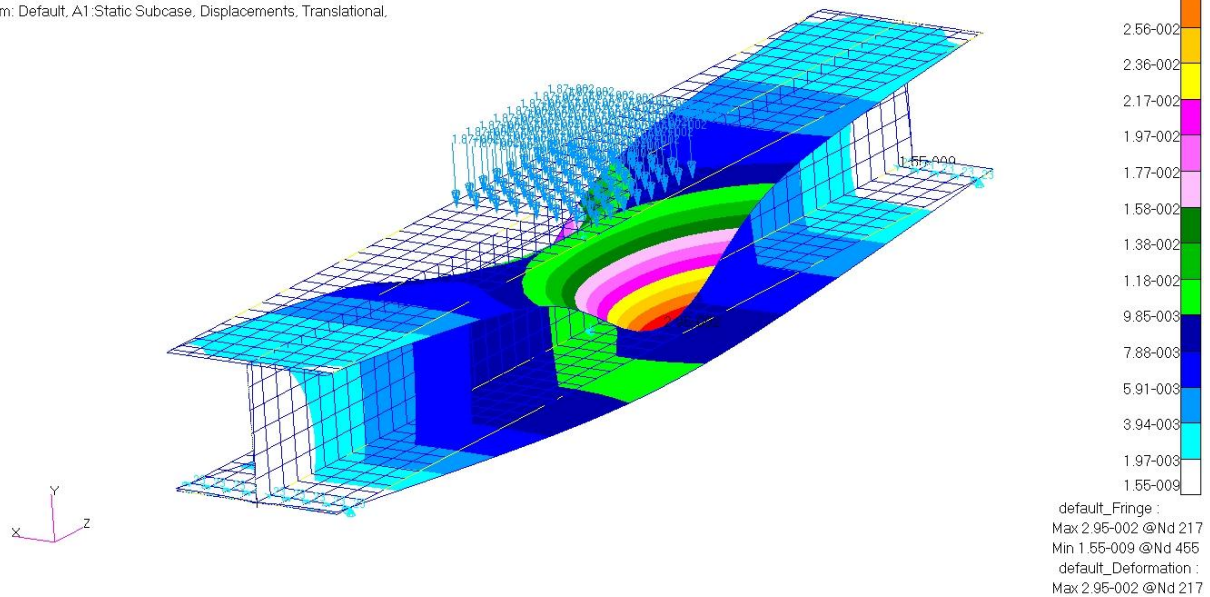
Deform: Default, A1:Static Subcase, Constraint Forces, Translational,



Patran 2008r2 30-May-11 11:40:14

Fringe: Default, A1:Static Subcase, Displacements, Translational, Magnitude, (NON-LAYERED)

Deform: Default, A1:Static Subcase, Displacements, Translational,

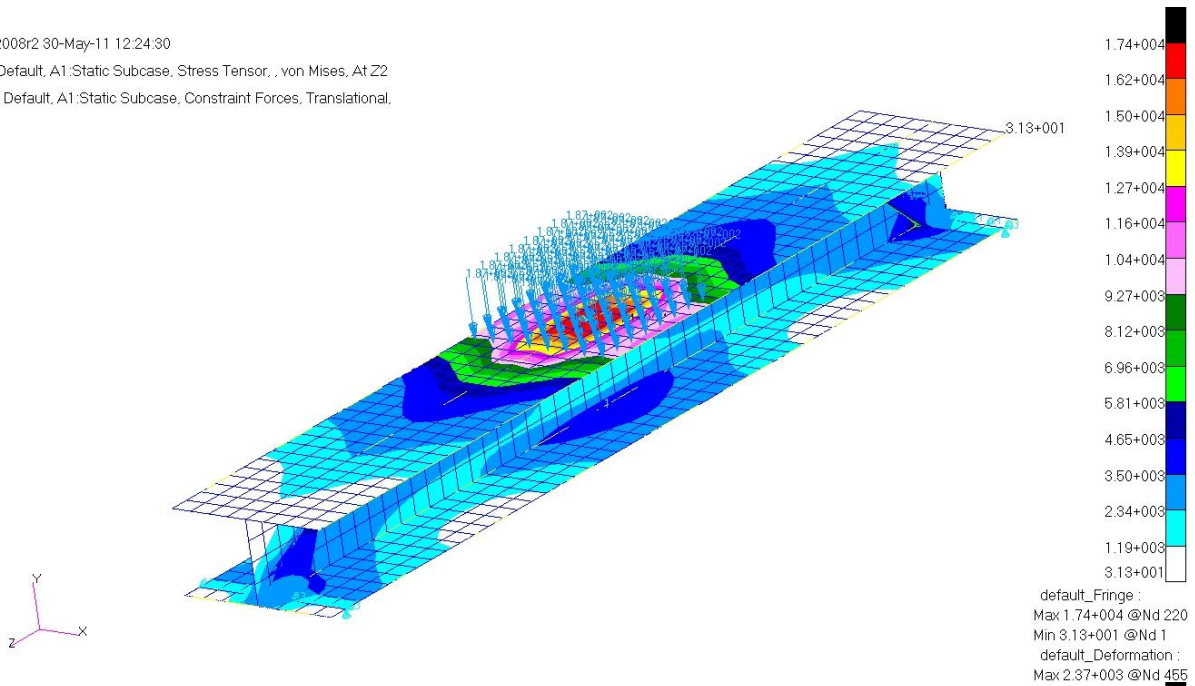


Appendix A.3 – Stress and Displacement Plots of Finite Element Model with 7075 Aluminum and 2 Inch Web

Patran 2008r2 30-May-11 12:24:30

Fringe: Default, A1:Static Subcase, Stress Tensor, , von Mises, At Z2

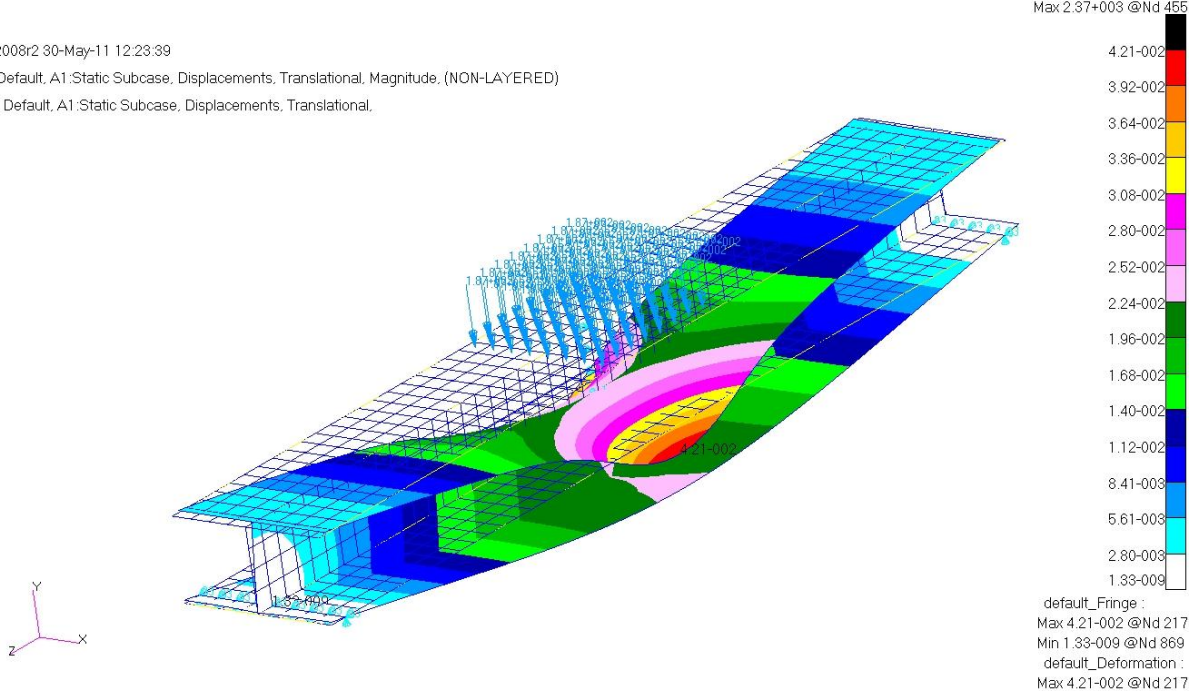
Deform: Default, A1:Static Subcase, Constraint Forces, Translational,



Patran 2008r2 30-May-11 12:23:39

Fringe: Default, A1:Static Subcase, Displacements, Translational, Magnitude, (NON-LAYERED)

Deform: Default, A1:Static Subcase, Displacements, Translational,

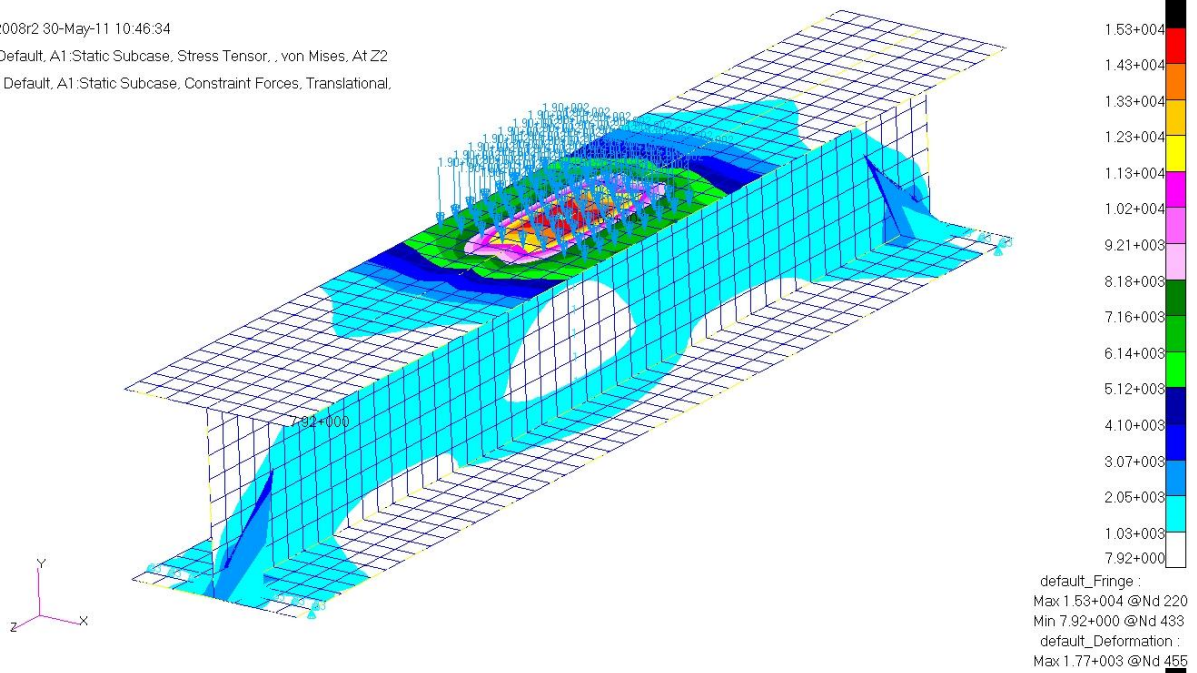


Appendix A.4 – Stress and Displacement Plots of Finite Element Model with 4130 Steel and 4 Inch Web

Patran 2008r2 30-May-11 10:46:34

Fringe: Default, A1:Static Subcase, Stress Tensor, von Mises, At Z2

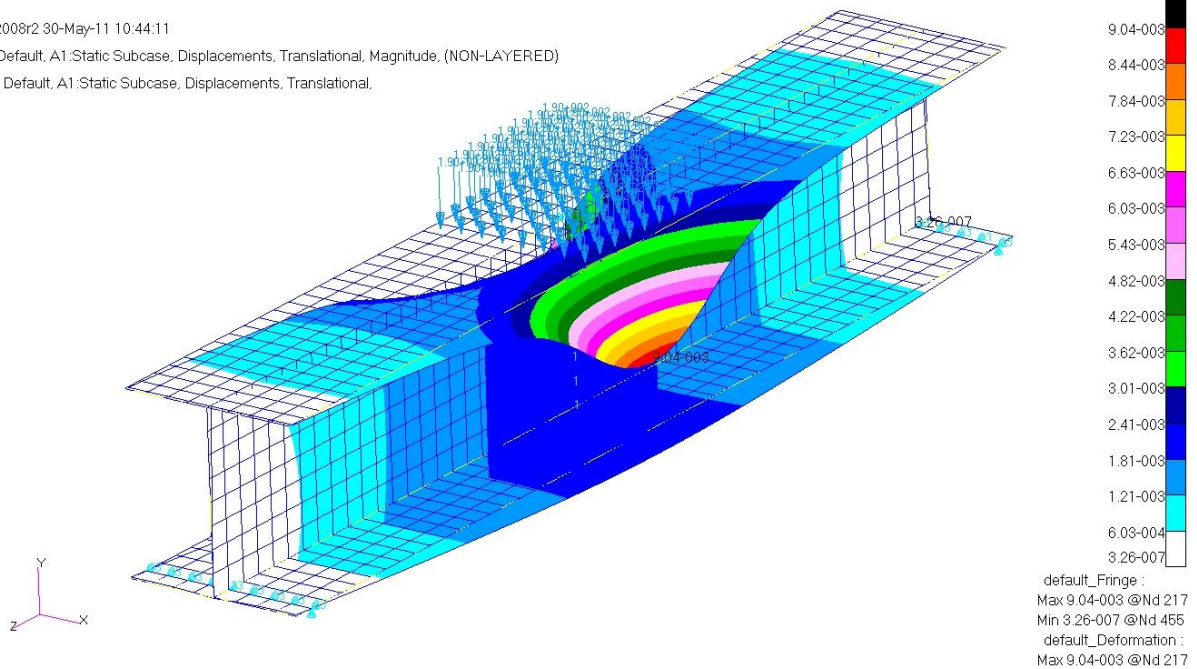
Deform: Default, A1:Static Subcase, Constraint Forces, Translational,



Patran 2008r2 30-May-11 10:44:11

Fringe: Default, A1:Static Subcase, Displacements, Translational, Magnitude, (NON-LAYERED)

Deform: Default, A1:Static Subcase, Displacements, Translational,

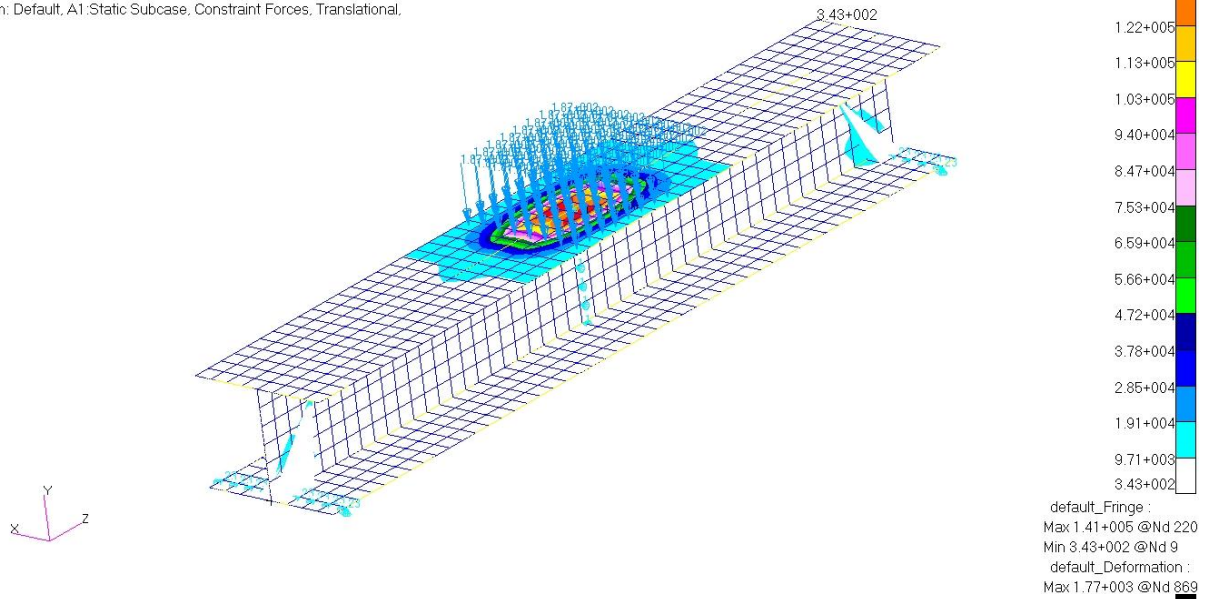


Appendix A.5 – Stress and Displacement Plots of Finite Element Model with 4130 Steel and 3 Inch Web

Patran 2008r2 30-May-11 12:03:48

Fringe: Default, A1:Static Subcase, Stress Tensor, von Mises, Layer 1

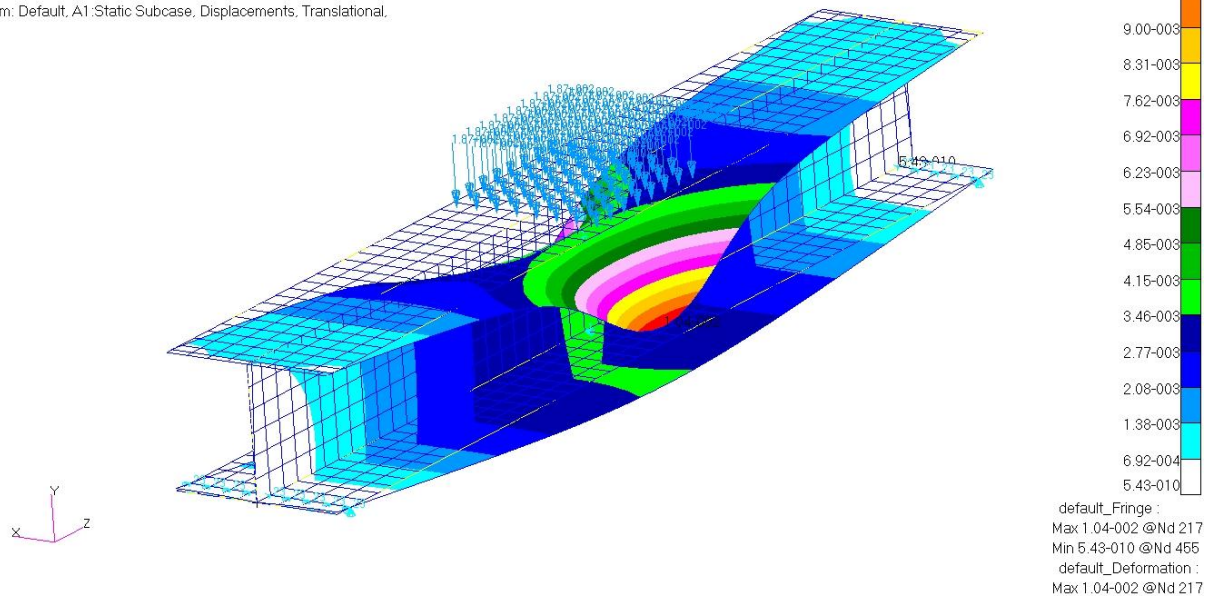
Deform: Default, A1:Static Subcase, Constraint Forces, Translational,



Patran 2008r2 30-May-11 11:52:11

Fringe: Default, A1:Static Subcase, Displacements, Translational, Magnitude, (NON-LAYERED)

Deform: Default, A1:Static Subcase, Displacements, Translational,

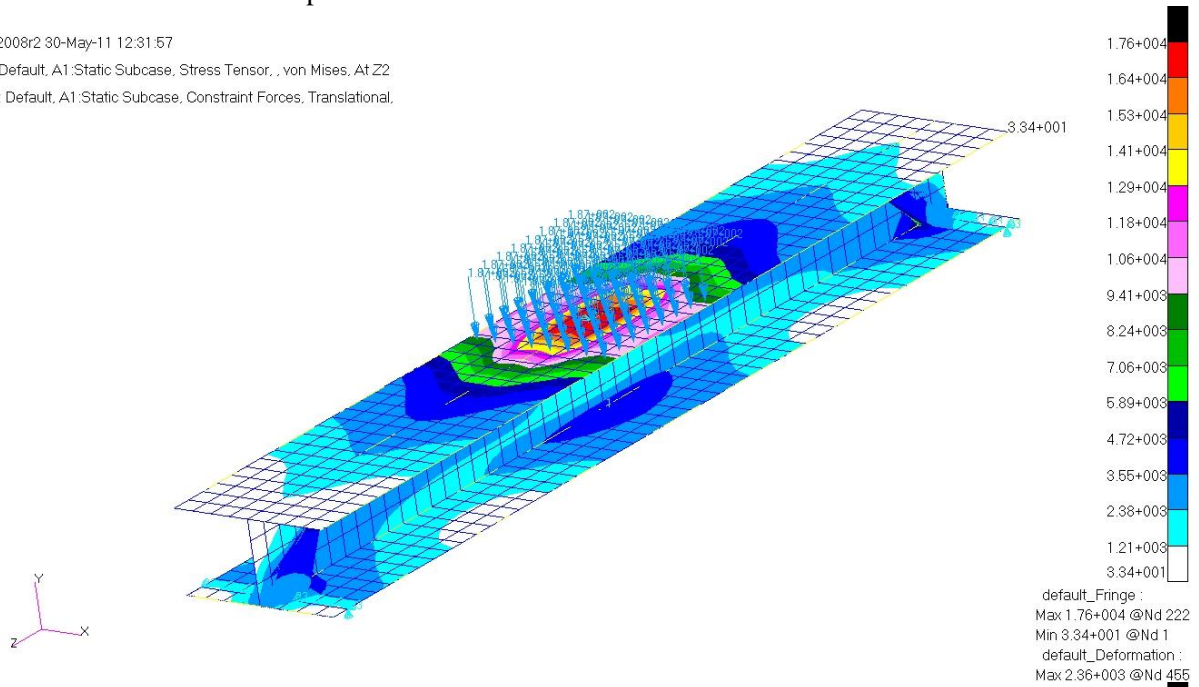


Appendix A.6 – Stress and Displacement Plots of Finite Element Model with 4130 Steel and 2 Inch Web

Patran 2008r2 30-May-11 12:31:57

Fringe: Default, A1:Static Subcase, Stress Tensor, von Mises, At Z2

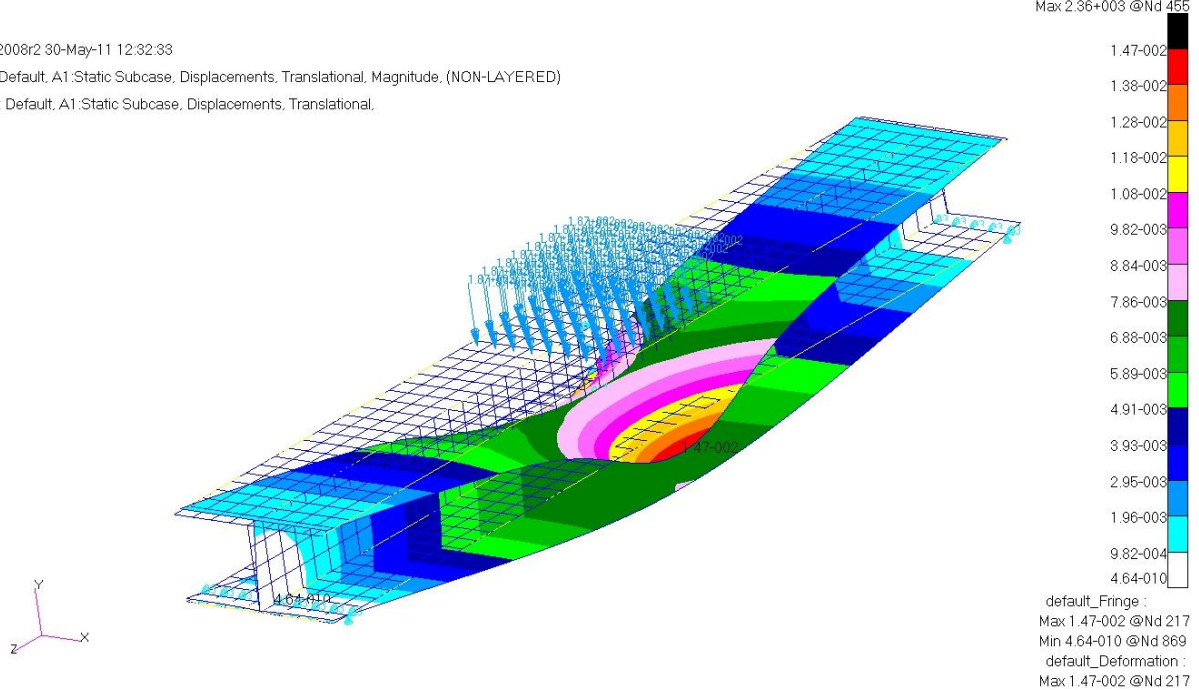
Deform: Default, A1:Static Subcase, Constraint Forces, Translational,



Patran 2008r2 30-May-11 12:32:33

Fringe: Default, A1:Static Subcase, Displacements, Translational, Magnitude, (NON-LAYERED)

Deform: Default, A1:Static Subcase, Displacements, Translational,

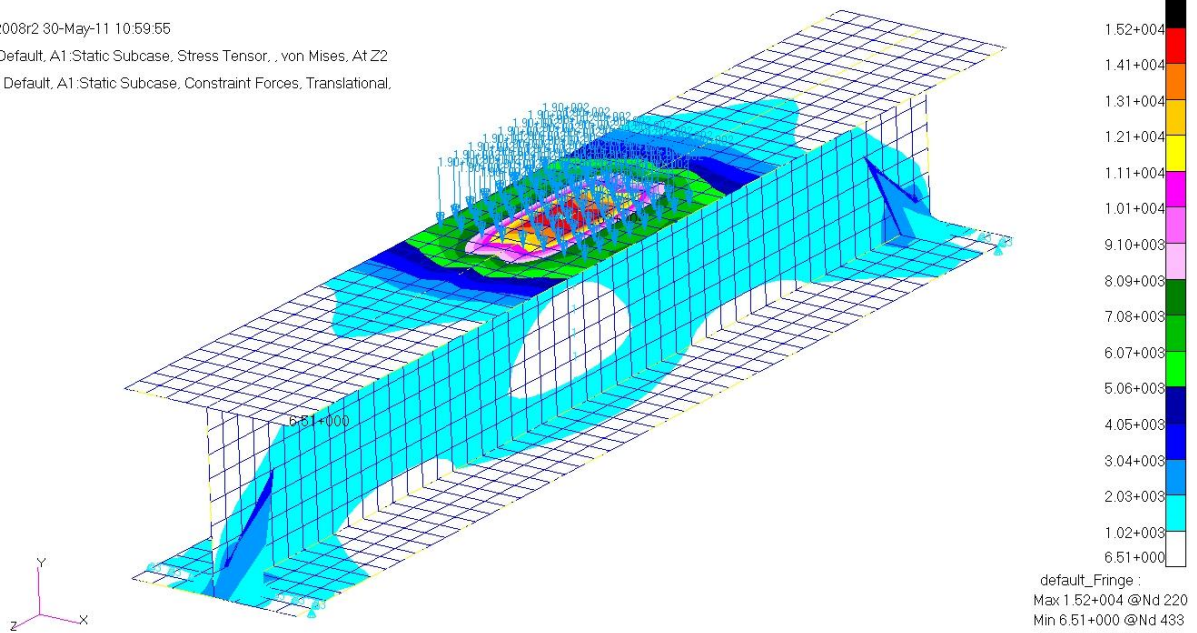


Appendix A.7 – Stress and Displacement Plots of Finite Element Model with Ti 6Al-4V Titanium and 4 Inch Web

Patran 2008r2 30-May-11 10:59:55

Fringe: Default, A1:Static Subcase, Stress Tensor, , von Mises, At Z2

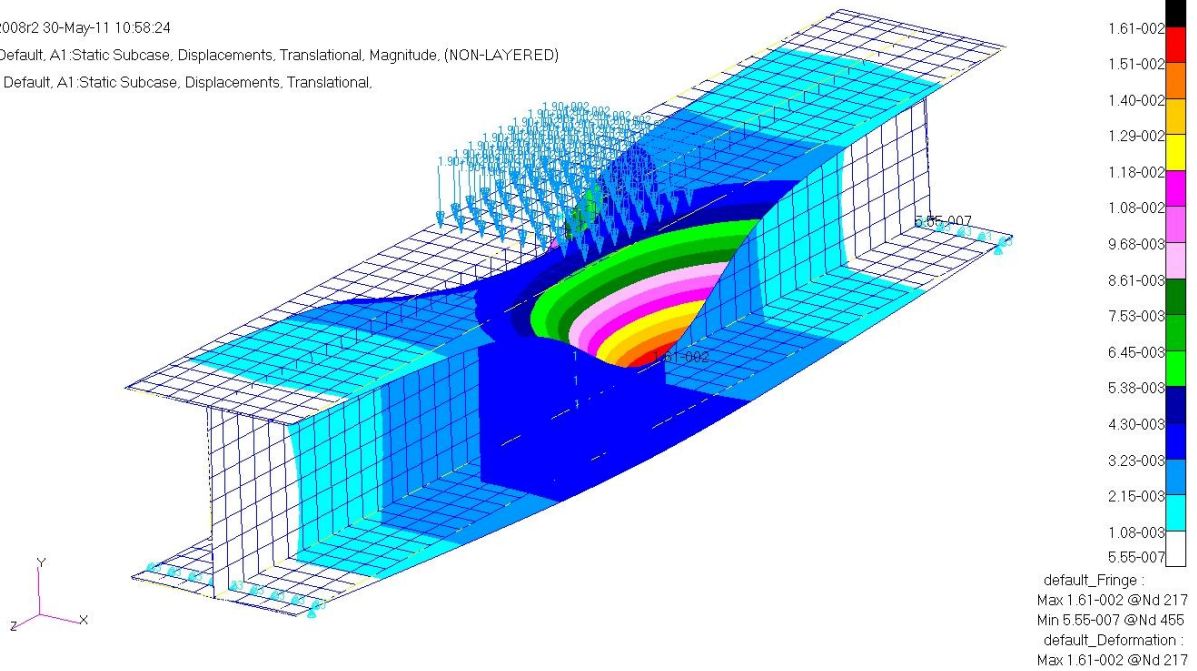
Deform: Default, A1:Static Subcase, Constraint Forces, Translational,



Patran 2008r2 30-May-11 10:58:24

Fringe: Default, A1:Static Subcase, Displacements, Translational, Magnitude, (NON-LAYERED)

Deform: Default, A1:Static Subcase, Displacements, Translational,

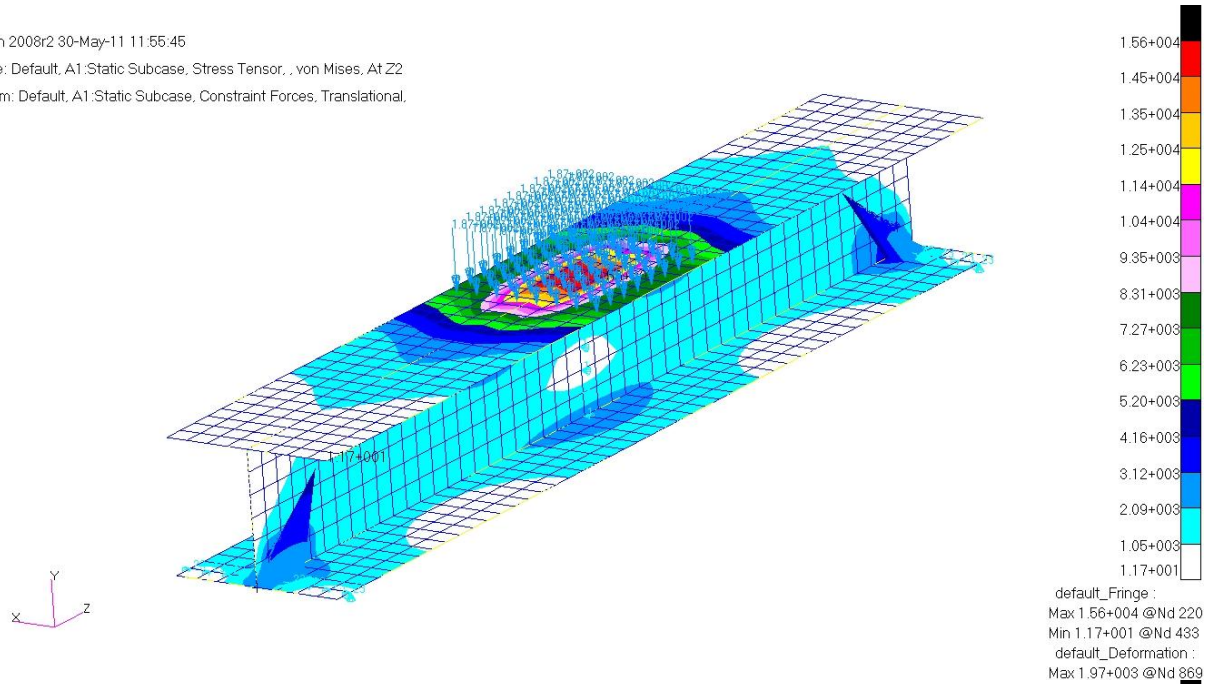


Appendix A.8 – Stress and Displacement Plots of Finite Element Model with Ti 6Al-4V Titanium and 3 Inch Web

Patran 2008r2 30-May-11 11:55:45

Fringe: Default, A1:Static Subcase, Stress Tensor, von Mises, At Z2

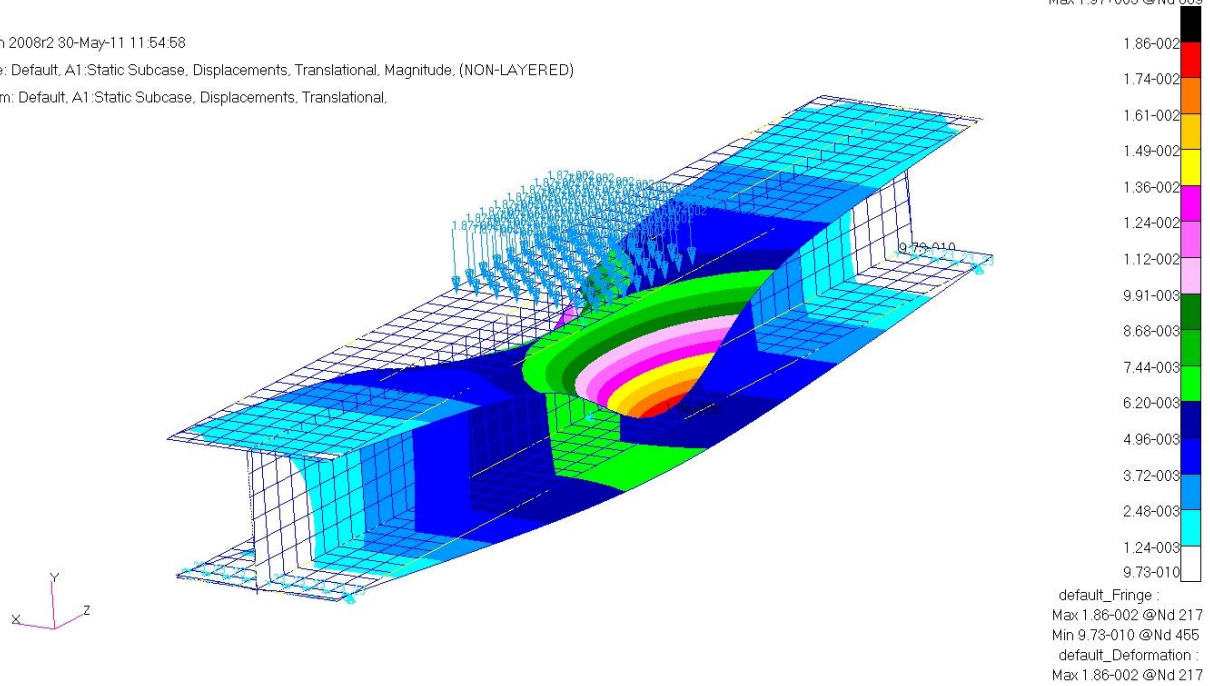
Deform: Default, A1:Static Subcase, Constraint Forces, Translational,



Patran 2008r2 30-May-11 11:54:58

Fringe: Default, A1:Static Subcase, Displacements, Translational, Magnitude, (NON-LAYERED)

Deform: Default, A1:Static Subcase, Displacements, Translational,

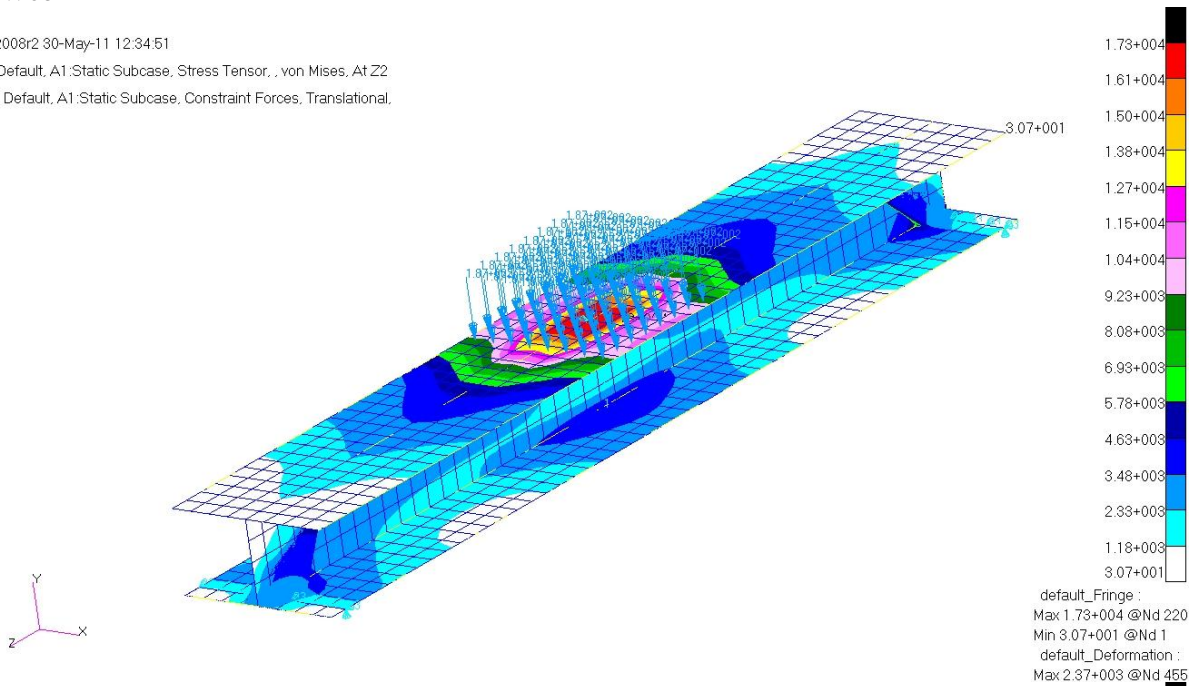


Appendix A.9 – Stress and Displacement Plots of Finite Element Model with Ti 6Al-4V Titanium and 2 Inch Web

Patran 2008r2 30-May-11 12:34:51

Fringe: Default, A1:Static Subcase, Stress Tensor, , von Mises, At Z2

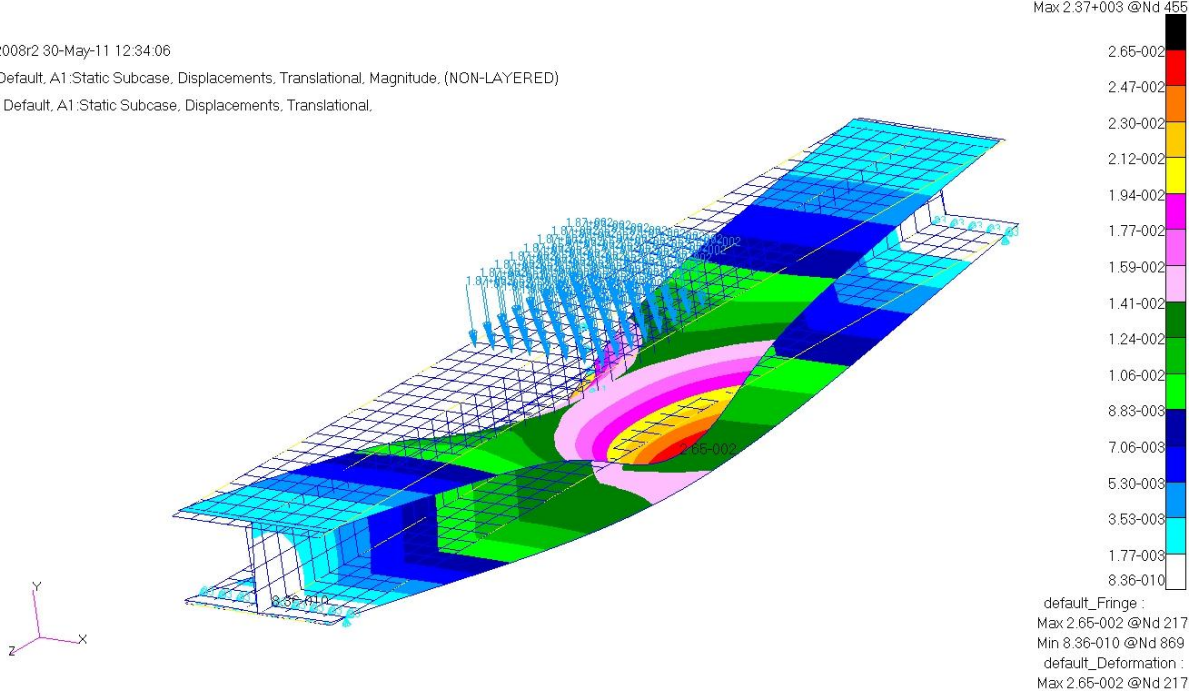
Deform: Default, A1:Static Subcase, Constraint Forces, Translational,



Patran 2008r2 30-May-11 12:34:06

Fringe: Default, A1:Static Subcase, Displacements, Translational, Magnitude, (NON-LAYERED)

Deform: Default, A1:Static Subcase, Displacements, Translational,

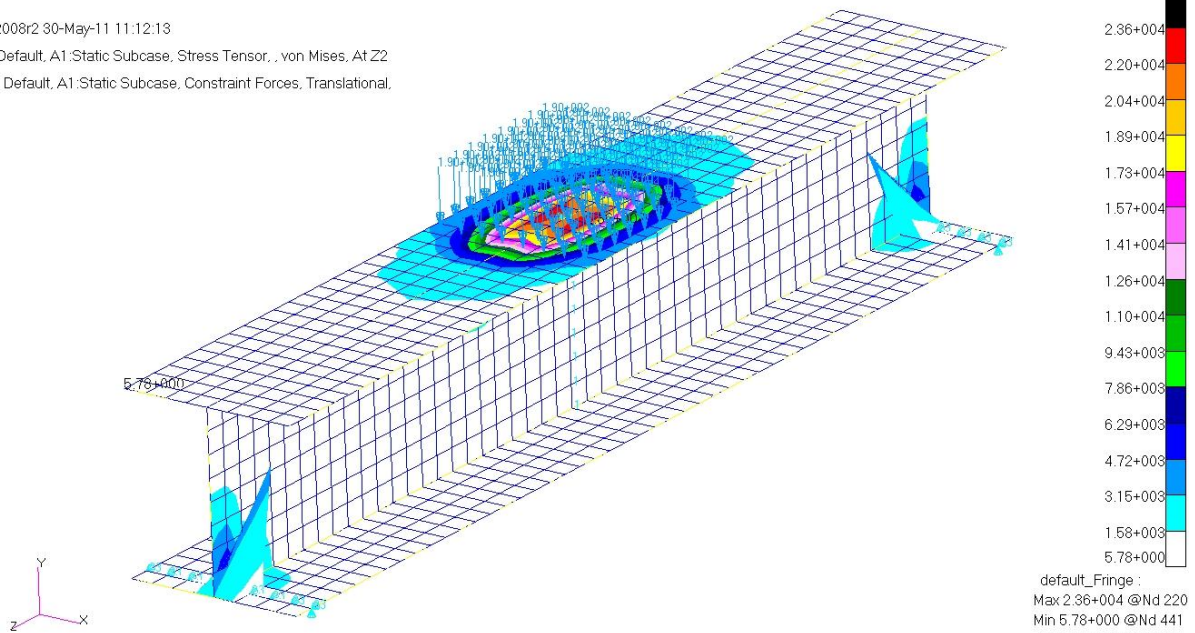


Appendix A.10 – Stress and Displacement Plots of Finite Element Model with Woven Carbon Fiber and 4 Inch Web

Patran 2008r2 30-May-11 11:12:13

Fringe: Default, A1:Static Subcase, Stress Tensor, , von Mises, At Z2

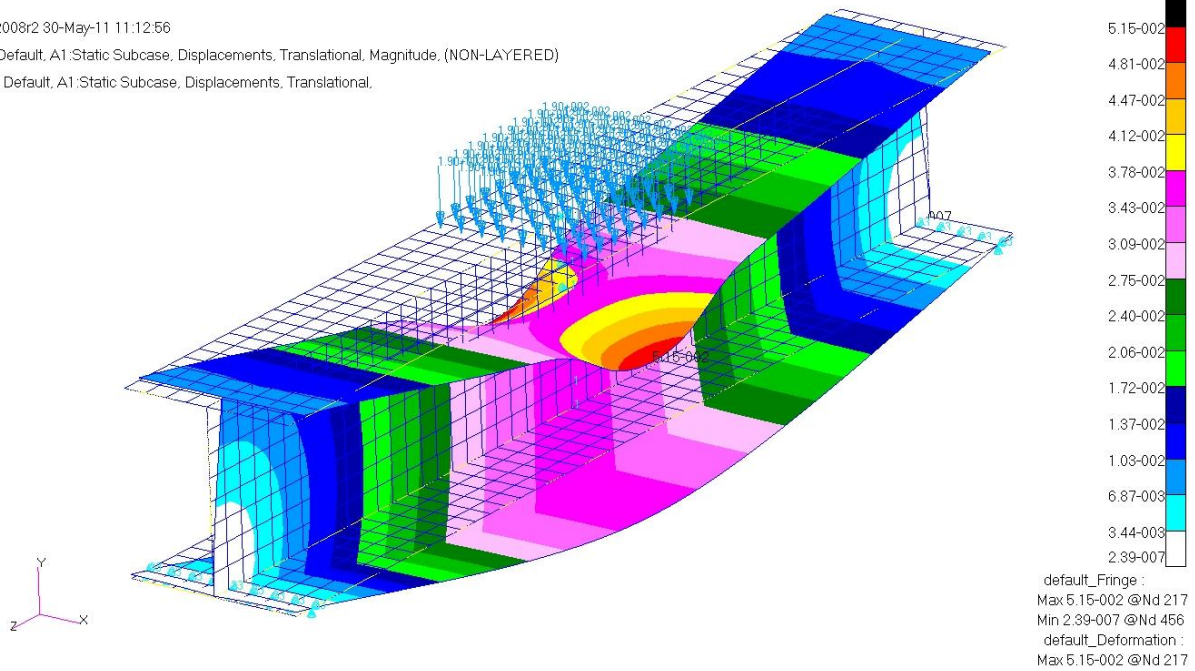
Deform: Default, A1:Static Subcase, Constraint Forces, Translational,



Patran 2008r2 30-May-11 11:12:56

Fringe: Default, A1:Static Subcase, Displacements, Translational, Magnitude, (NON-LAYERED)

Deform: Default, A1:Static Subcase, Displacements, Translational,

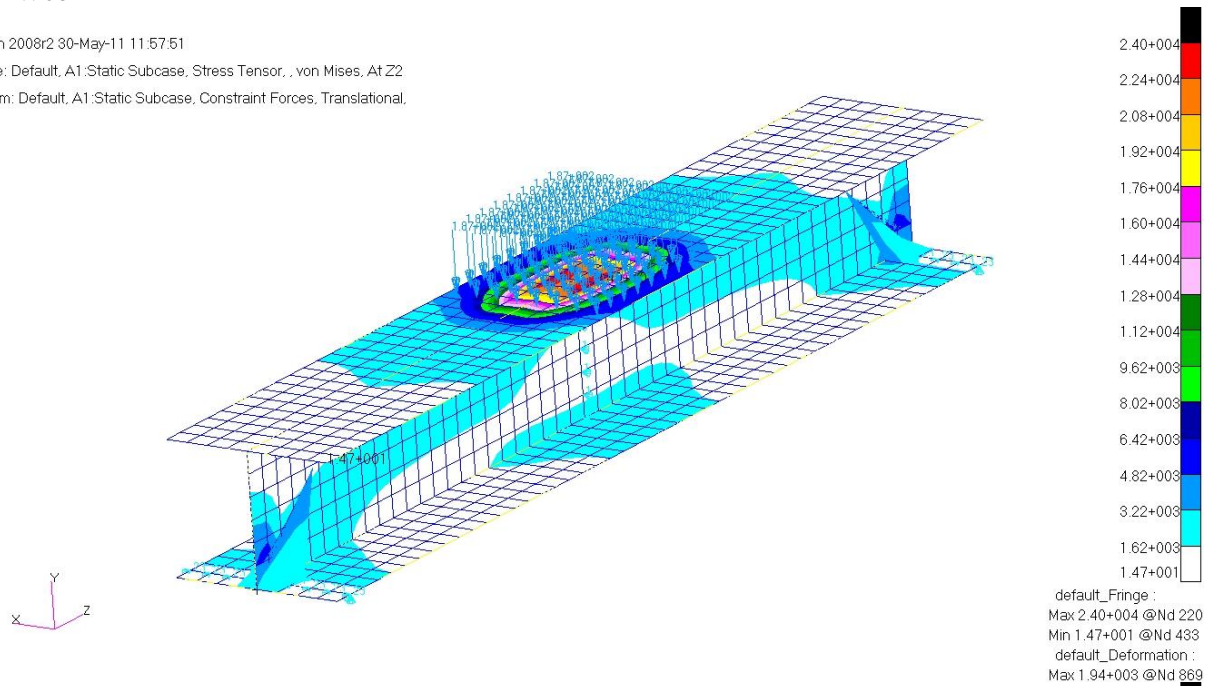


Appendix A.11 – Stress and Displacement Plots of Finite Element Model with Woven Carbon Fiber and 3 Inch Web

Patran 2008r2 30-May-11 11:57:51

Fringe: Default, A1:Static Subcase, Stress Tensor, , von Mises, At Z2

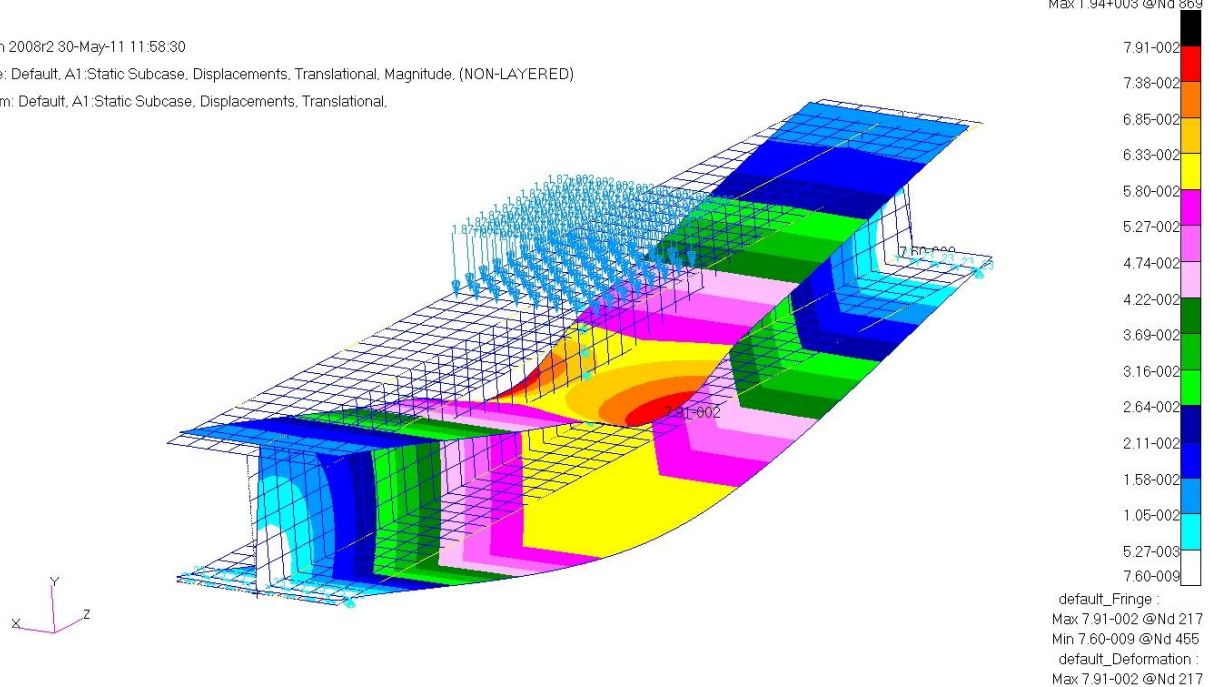
Deform: Default, A1:Static Subcase, Constraint Forces, Translational,



Patran 2008r2 30-May-11 11:58:30

Fringe: Default, A1:Static Subcase, Displacements, Translational, Magnitude, (NON-LAYERED)

Deform: Default, A1:Static Subcase, Displacements, Translational,

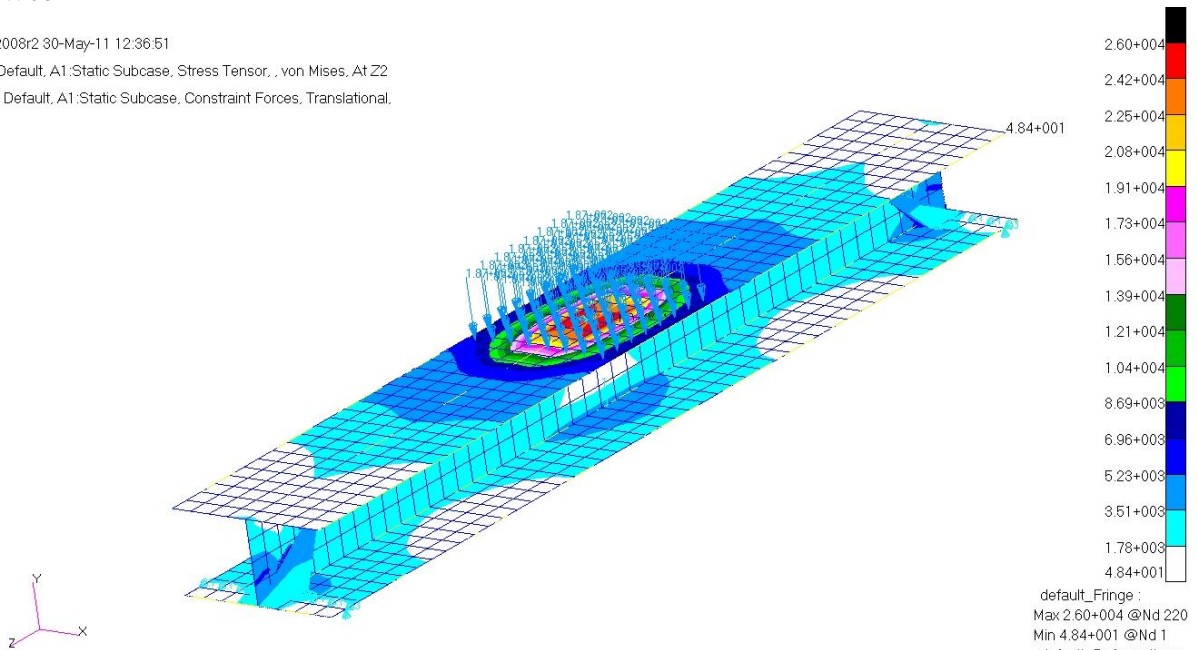


Appendix A.12 – Stress and Displacement Plots of Finite Element Model with Woven Carbon Fiber and 2 Inch Web

Patran 2008r2 30-May-11 12:36:51

Fringe: Default, A1:Static Subcase, Stress Tensor, , von Mises, At Z2

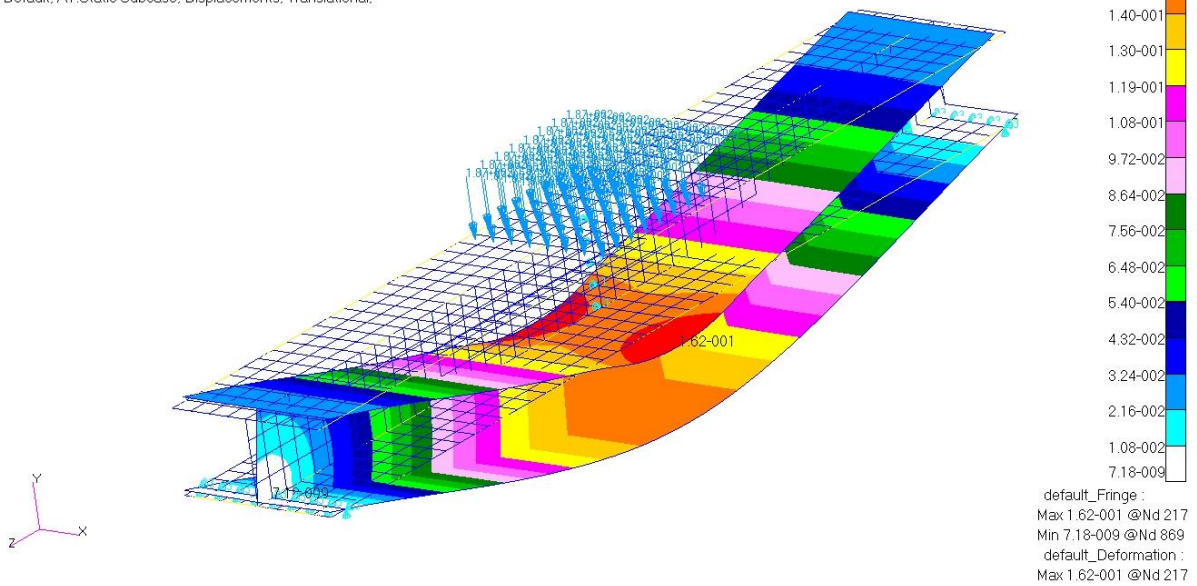
Deform: Default, A1:Static Subcase, Constraint Forces, Translational,



Patran 2008r2 30-May-11 12:37:23

Fringe: Default, A1:Static Subcase, Displacements, Translational, Magnitude, (NON-LAYERED)

Deform: Default, A1:Static Subcase, Displacements, Translational,



Appendix A.13 – MATLAB Code used for Classical Beam Theory Analysis

```
%%%%%%%%%%%%%%%%%%%%%%%%%%%%%%%%%%%%%%%%%%%%%%%%%%%%%%%%%%%%%%%%%%%%%%%%%%%%%%
% Kodi Rider
% Sr. Project - Classical Beam Calcs
% 4 June 2011
%%%%%%%%%%%%%%%%%%%%%%%%%%%%%%%%%%%%%%%%%%%%%%%%%%%%%%%%%%%%%%%%%%%%%%%%%%%%%%

close all;
clear all;
clc;

%% Constants
E = [10.4e6 29.7e6 16.5e6];
%Elastic modulus of [7075 Aluminum, 4130 Steel, Ti 6Al-4V Titanium] (psi)

t = 0.25; %assumed flange thickness (in)
base = 4; %assumed flange width (in)

t_web = 0.6; %assumed web thickness (in)
h_web = [4 3.5 3]; %varied web height (in)

P = 3000; %total load applied to bridge (lbf)
L = 23; %total I-beam length (in)
%% Calcs

a = 9.5; %distance from roller support to load (inches)
c = a;
b = 4; %length of distributed load (inches)
x = 11.5; %distance from roller support to center of bridge (inches)
w = P/b; %applied distributed

for i = 1:length(h_web)
    I(i) = (1/12)*((base*(h_web(i)+(2*t))^3)-((base-t_web)*h_web(i)^3));...
    %moment of inertia (in^4)
    for j = 1:length(E)
        dmax(i,j) = (w/(24*E(j)*I(i)))*((base*(base+(2*c))*x)/L)*...
        ((-2*x^2)+((2*a)*((2*L)-a)))+(base*(base+(2*c))));...
        %maximum displacement (inches)
    end
end
end
```

Acknowledgments

We would like to thank Dr. Eltahry I. Elghandour for providing us a chance to physically practice the structural theory that we have learned in class.

We would also like to thank the lab technician, Michael Jacobson, for assisting us in manufacturing our composite beams and having everything in the lab working as they should.

References

- ¹Jones, R., "Mechanics of Composite Materials," 2nd Edition, Taylor & Francis, Philadelphia, PA, 1999.
- ²Engineer's Handbook, "Manufacturing Processes - Autoclave Molding," 2004,
<http://www.engineershandbook.com/MfgMethods/autoclavemolding.htm>.
- ³Savic, V., Tuttle, M., Zabinsky, Z., "Optimization of Composite I-sections Using Fiber Angles as Design Variables," Composite Structures, 2001.
- ⁴AvPro, "Autoclave," <http://www.avproinc.com/Autoclave.jpg>.
- ⁵Diaz, J., Grant, C., Grimshaw, M., "Advanced Technology Tape Laying for Affordable Manufacturing of Large Composite Structures."
- ⁶M. D. Gilchrist, A. J. Kinloch, F. L. Matthews and S. O. Osiyemi, "Mechanical Performance of Carbon-Fibre and Glass-Fibre reinforced epoxy I-beams: I. Mechanical behaviour," ScienceDirect, Feb, 2011, Composites Science and Technology, Vol. 56, Issue 1, 1996, Pages 37-53.
- ⁷K. D. Potter, R. Davies, M. Barrett, L. Bateup, M. Wisnom and A. Mills, "Heavily loaded bonded composite structure: design, manufacture and test of "I" beam specimens," ScienceDirect, Feb, 2011, Composites Structures, Vol. 51, Issue 4, 2001, Pages 389-399.
- ⁸G.Zhou and J. Hood, "Design, manufacture and evaluation of laminated carbon/epoxy I-beams in bending," ScienceDirect, Feb, 2011, Composites Part A: Applied Science and Manufacturing, Vol. 37, Issue 3, 2006, Pages 506-517.
- ⁹Railsback. "Organic and Inorganic Compounds." *University of Georgia*. Department of Geology. Web. 11 Feb. 2011. <<http://www.gly.uga.edu/railsback/Fundamentals/SFMGOrganicInorganic06-I.pdf>>.
- ¹⁰"Boeing 787 From the Ground Up." *Boeing*. Web. 11 Feb. 2011.
 <http://www.boeing.com/commercial/aeromagazine/articles/qtr_4_06/article_04_2.html>.
- ¹¹"Carbon Fabric - Classic Styles." *Fibre Glast Developments : Carbon Fiber : Fiberglass : Resin : Kevlar : Epoxy : Polyester : Gel Coats : Fillers*. Web. 11 Feb. 2011. <<http://www.fibreglast.com/category/155>>.
- ¹²"Thermoplastic Composites Explained." *Eire Composites*. Web. 11 Feb. 2011.
 <http://www.eirecomposites.com/Thermoplastic_Composites_Explained.asp>.
- ¹³"Thermoset Composites." *Machine Design*. 15 Nov. 2002. Web. 11 Feb. 2011.
 <<http://machinedesign.com/article/thermoset-composites-1115>>.

- ¹⁴“AISI 4130 Steel Properties.” *Aerospace Specification Metals, Inc.* 30 May 2011. Web.
<<http://asm.matweb.com/search/SpecificMaterial.asp?bassnum=m4130r>>.
- ¹⁵“Titanium Ti-6Al-4V Properties.” *Aerospace Specification Metals, Inc.* 30 May 2011. Web.
<<http://asm.matweb.com/search/SpecificMaterial.asp?bassnum=MTP641>>.
- ¹⁶“7075 T6 Aluminum Properties.” *Aerospace Specification Metals, Inc.* 30 May 2011. Web.
<<http://asm.matweb.com/search/SpecificMaterial.asp?bassnum=MA7075T6>>.
- ¹⁷Blacketter, D.M., Walrath, D.E., Hansen, A.C., "Modeling Damage in a Plain Weave Fabric-Reinforced Composite Material", *Journal of Composites Technology & Research*, Vol. 15, No. 2, 1993, pp. 136-142.
- ¹⁸“Beam Formula.pdf.” *Engineering Tips*. 4 June 2011. Web.
<http://files.engineering.com/getfile.aspx?folder=d28c596c-1598-4491-99ae-98e7ca1baf73&file=Beam_Formula.pdf>.
- ¹⁹“SAMPE 2011 Student Bridge Contest.” SAMPE Website 2011. Web. 1 Feb 2011.
<<http://www.sampe.org/events/SAMPEStudentBridgeContest.aspx>>.